Streaming High-Quality Mobile Video with Multipath TCP in Heterogeneous Wireless Networks

Jiyan Wu, *Member, IEEE*, Chau Yuen, *Senior Member, IEEE*,
Bo Cheng, *Member, IEEE*, Ming Wang, and Junliang Chen

Abstract—The proliferating wireless infrastructures with complementary characteristics prompt the bandwidth aggregation for concurrent video transmission in heterogeneous access networks. Multipath TCP (MPTCP) is an important transport-layer protocol recommended by IETF to integrate different access medium (e.g., Cellular and Wi-Fi). This paper investigates the problem of mobile video delivery using MPTCP in heterogeneous wireless networks with multihomed terminals. To achieve the optimal quality of real-time video streaming, we have to seriously consider the path asymmetry in different access networks and the disadvantages of the data retransmission mechanism in MPTCP. Motivated by addressing these critical issues, this study presents a novel quAlity-Driven MultIpath TCP (ADMIT) scheme that integrates the utility maximization based Forward Error Correction (FEC) coding and rate allocation. We develop an analytical framework to model the MPTCP-based video delivery quality over multiple communication paths. ADMIT is able to effectively integrate the most reliable access networks with FEC coding to minimize the end-to-end video distortion. The performance of ADMIT is evaluated through extensive semi-physical emulations in Exata involving H.264 video streaming. Experimental results show that ADMIT outperforms the reference transport protocols in terms of video PSNR (Peak Signal-to-Noise Ratio), end-to-end delay, and goodput. Thus, we recommend ADMIT for streaming high-quality mobile video in heterogeneous wireless networks with multihomed terminals.

Index Terms—Quality-driven, multipath TCP, real-time mobile video, heterogeneous wireless networks, forward error correction, multihomed communication

1 Introduction

Recent advancements in the network infrastructures and communication technologies of wireless systems provide ubiquitous access options for mobile users (e.g., LTE, Wi-Fi, HSDPA, 3G, etc.) [1], [2], [3], [4]. As these different wireless networks have complementary characteristics, it is desirable for the individual mobiles to establish multiple simultaneous associations to improve data throughput and transmission reliability [5], [6]. With the prevalence of multihomed terminals (e.g., the Samsung S5 smart cell phones [7] and Mushroom products [8]), the future wireless environment is envisioned to be a converged system that incorporates heterogeneous access networks for providing high-quality mobile services. Therefore, new research trends [9], [10], [11] have moved towards integrating the heterogeneous access networks with Multipath TCP (MPTCP) [12], which is the transport-layer protocol recommended by IETF (Internet Engineering Task Force) to enable parallel data transfer (as shown in Fig. 1).

- *J. Wu, B. Cheng, M. Wang and J. Chen are with the State Key Laboratory of Networking and Switching Technology, Beijing University of Posts and Telecommunications, Beijing 100876, P. R. China. E-mail: {wujiyan, chengbo, wangming_bupt, chjl}@bupt.edu.cn.*
- *C. Yuen is with the Engineering Product Development Pillar, Singapore University of Technology and Design, 8 Somapah Road, Singapore 487372, Republic of Singapore. E-mail: yuenchau@sutd.edu.sg.*

Manuscript received 2 June 2015; revised 26 Oct. 2015; accepted 29 Oct. 2015. Date of publication 3 Nov. 2015; date of current version 2 Aug. 2016.
For information on obtaining reprints of this article, please send e-mail to: reprints@ieee.org, and reference the Digital Object Identifier below.
Digital Object Identifier no. 10.1109/TMC.2015.2497238

Prompted by the radical evolutions in wireless infrastructures, mobile video streaming has already become the most popular applications over the past few years. The latest market research conducted by Cisco company indicates video traffic accounts for 55 percent of the total mobile data usage over the Internet in 2014 and will reach 72 percent by the year 2019 [13]. Global mobile data is expected to increase 10-fold from 2014 to 2019. As the throughput demand of high-quality video streaming outpaces the available capacity in single wireless networks, it is important to exploit the multihoming feature of mobile devices to integrate different access networks. MPTCP is a promising transport-layer protocol to support multihomed video delivery in heterogeneous wireless environments.

Real-time video communication is one of the key research issues in multimedia delivery using TCP-based protocols (e.g., Web Real-Time Communication [14], HTTP live streaming [15], Skype, cloud gaming [16], etc.). Real-time Transport Protocol (RTP) [17] and Real-time Streaming Protocol (RTSP) [18] are also widely used for streaming real-time video. However, these protocols do not possess the special features of TCP, e.g., in firewall traversal and network friendliness. Despite the perceived advantages of MPTCP, it still remains problematic to deliver high-quality live video streaming with this transport protocol in heterogeneous wireless networks. The main reasons are three-fold [10], [19], [20], [21], [22], [23]:

1) *Data retransmission*. MPTCP is a connection-oriented protocol and achieves reliability with data retransmissions. However, this error control mechanism

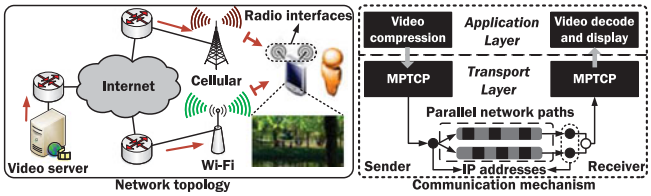

Fig. 1. Network topology and communication mechanism for multihomed video transmission with MPTCP over heterogeneous wireless networks.

ignores the delay constraint imposed by real-time video applications. The overdue packets cannot contribute to the decoding process even if they are successfully retransmitted.

2) *Congestion control*. The congestion window sizes in MPTCP are adapted in a additively increased and multiplicatively decreased fashion [10], [24]. Such congestion control strategy results in the frequent throughput fluctuations and significantly increases the end-to-end delay.
3) *Path asymmetry*. Different physical properties result in the path asymmetry of heterogeneous wireless networks. Involving an asymmetry communication path in multipath video communication may degrade the overall streaming quality.

To address these critical issues, this study presents a quAlity-Driven MultIpath TCP (ADMIT) to enable smooth live video streaming with following solutions: 1) employs the Forward Error Correction (FEC) coding to remedy the shortcoming of packet retransmission for protecting video data within stringent delay constraint (Section 4.1); 2) analyzes the MPTCP connection state to mitigate throughput fluctuations (Section 3.2); 3) delivers video streaming over the communication paths with regard to the reliability (Section 4.2).

Compared with the existing studies in MPTCP [9], [10], [11], we advance the state of the art by introducing a quality-driven optimization framework into the decision process of multipath data transfer. This framework comprehensively analyzes the video quality characteristics, end-to-end connection delay, and time-varying wireless channel status. We analytically formulate the constrained optimization problem of joint FEC coding and rate allocation to minimize the end-to-end video distortion. Then, we present a utility maximization framework for online adaption of FEC coding parameters and flow rate allocation. ADMIT is able to effectively integrate the most reliable wireless access networks with FEC coding to maximize the video quality. The detailed descriptions of the proposed ADMIT will be presented in Section 4.

In particular, the contributions of this study are threefold.

- Develop an analytical framework to model the end-to-end distortion of real-time video communication with MPTCP over multiple wireless access networks.
- Propose a MPTCP scheme dubbed ADMIT that effectively integrates the following components
  1) A reliability-aware flow rate allocation algorithm to dynamically select appropriate access networks to maximize the video quality.
  2) A utility-maximization based FEC coding scheme to strike the balance between delay and loss performance to minimize the effective packet loss rate (PLR).
- Perform extensive semi-physical emulations over the Exata platform involving H.264 video streaming. Evaluation results demonstrate that:
  1) ADMIT improves the average video PSNR by up to 5.8 (18.2 percent), 7.6 (23.3 percent), 9.7 (31.7 percent), and 12.1 (37.5 percent) dB compared to the GreenBag [25], FMTCP [21], MPLOT [26], and MPTCP [12].
  2) ADMIT reduces the average end-to-end delay by up to 22.3 (20.7 percent), 33.7 (27.2 percent), 48.7 (35.2 percent), and 65.1 (43.6 percent) ms compared to the GreenBag, FMTCP, MPLOT and MPTCP, respectively.
  3) ADMIT increases the mean goodput values by up to 0.13 (11.3 percent), 0.19 (15.3 percent), 0.25 (19.1 percent), and 0.31 (22.6 percent) Mbps compared to the GreenBag, FMTCP, MPLOT and MPTCP, respectively.

The remainder of this paper is structured as follows. Section 2 briefly reviews the related work to this paper. In Section 3, we present the system model and problem formulation. Section 4 introduces the solution procedure of the proposed ADMIT in detail. The performance evaluation is provided in Sections 5 and 6 gives the concluding remarks of this work.

2 Related Work

The related work to this study can be classified into two categories: 1) multihomed video communication in heterogeneous wireless networks; 2) MPTCP solutions.

2.1 Multihomed Video Communication

Han et al. [6] propose an end-to-end virtual path construction system over heterogeneous wireless networks based on fountain code. The goal of this system is to maximize the video encoding bit rate on the basis of aggregate bandwidth, as well as overcoming the channel loss. In literature [27], the authors propose a sub-frame level (SFL) scheduling approach, which splits large-size video frames to optimize the delay performance of HD video streaming over heterogeneous wireless networks. Song and Zhuang [28] present a Probabilistic Multipath Transmission (PMT) scheme, which sends video traffic bursts over multiple available paths based on a probability generation function of packet delay. In [29], the authors introduce a dynamic rate allocation algorithm into joint source-channel coding (JSCC) to optimize the mobile video quality over heterogeneous networks. In [2], the authors propose a Distortion-Aware Concurrent Multipath Transfer scheme (CMT-DA) to minimize the end-to-end video distortion in mobile video delivery over heterogeneous wireless networks. However, CMT-DA still provides data protection with retransmissions and is not appropriate for delay-constrained video applications. Bui et al. [25] propose the GreenBag that includes the load balancing, segment management and energy-aware mode control to deliver mobile video over heterogeneous wireless

TABLE 1
Differences of the Proposed ADMIT with the Existing Works [2], [27], [29], [30]

	protocol layer	data protection	data/rate allocation	TCP connection state	FEC adaption
ADMIT	transport layer (MPTCP)	FEC, retransmission	reliability-aware	✓	redundancy, packet size
CMT-DA [2]	transport layer (SCTP)	retransmission	utility maximization	×	×
SFL [27]	application layer	×	water-filling	×	×
LTBA [30]	application layer	FEC	bandwidth-based	×	×
FRA-JSCC [29]	application-physical layer	FEC	greedy search	×	redundancy

networks. Xu et al. [3] propose a Quality-Aware Adaptive Concurrent Multipath Transfer (CMT-QA) scheme that includes the components of data distribution, path quality estimation and optimal retransmission. Specifically, the path quality is estimated with the sending buffer size and transmission delay. Wu et al. [34] propose a Content-Aware Concurrent Multipath Transfer scheme that performs priority-aware chunk scheduling in Stream Control Transmission Protocol (SCTP) to optimize the streaming quality. In [30], a Loss Tolerant Bandwidth Aggregation (LTBA) scheme is proposed to spread the FEC packets over multiple wireless networks to minimize the channel distortion. The differences of the proposed ADMIT with our earlier works [2], [27], [29], [30] are summarized in Table 1. ADMIT is different from the existing studies [2], [27], [29], [30] in the protocol type, data protection mechanism, rate allocation scheme, delay performance model, and FEC adaption algorithms.

2.2 MPTCP Solutions

Bonaventure et al. generally review the recent studies on MPTCP in literature [31]. The Request For Comments (RFC) of IETF to describe MPTCP is presented in reference [32]. The Fountain Code-based Multipath TCP (FMTCP) proposed by Cui et al. in literature [21] leverages the random nature fountain coding to overcome channel erasures and path heterogeneity in multipath data transfer. However, the video quality is not considered in [21] and this metric is significantly different from the network-level parameters (e.g., throughput, delay, packet loss rate, etc.). Furthermore, the block size of fountain code is too large, and thus is not effective for real-time video applications with stringent delay constraint. Li et al. [33] propose the SC-MPTCP scheme that introduces the linear systematic coding into MPTCP. SC-MPTCP addresses the problem of tolerating the path heterogeneity under receiver buffer limitation. The redundancy is provisioned into both proactive and reactive data. Chen et al. [9] propose an energy-efficient MPTCP scheme that leverages the throughput-energy tradeoff for path selection and congestion control. Chen et al. [9] conduct a measurement study of MPTCP performance over cellular and Wi-Fi networks to investigate the impact of path diversity on application-level metrics.

In summary, the challenging problem of MPTCP-based real-time video communication is not investigated in existing studies. *To the best of our knowledge, the proposed ADMIT is the first MPTCP scheme that incorporates the quality-driven FEC coding and rate allocation to achieve distortion-minimized video streaming in heterogeneous wireless networks.*

3 System Model and Problem Formulation

3.1 System Overview

The system overview of the proposed ADMIT framework is presented in Fig. 2. ADMIT is special version of MPTCP designed for streaming real-time high-quality video traffic. We consider the end-to-end transmission of a single video flow using the MPTCP connection over heterogeneous wireless access networks. The goal of the proposed ADMIT is to achieve the optimal-quality video streaming by adapting the FEC coding parameters and assigning the video transmission rate. The input video flow is divided into multiple sub-flows onto the available access networks. Each sub-flow is composed of several segments. In this study, we use the following two default settings of MPTCP.

Setting 1 (Full-MPTCP mode). Under the full-MPTCP mode [35], the traffic data can be concurrently transmitted through all the available communication paths.

Setting 2 (Coupled congestion control). This congestion control algorithm (linked increase algorithm [24]) couples the increases in congestion windows and decreases the window sizes by half (i.e., the multiplicative decrease pattern in TCP) should packet loss occurs.

The working components in the system design of ADMIT are implemented at both sender and receiver sides. The sender blocks include the parameter control unit, FEC coder, rate allocator, and data transmitter. In particular, the FEC redundancy (Algorithm 1) and packet size (Algorithm 2)

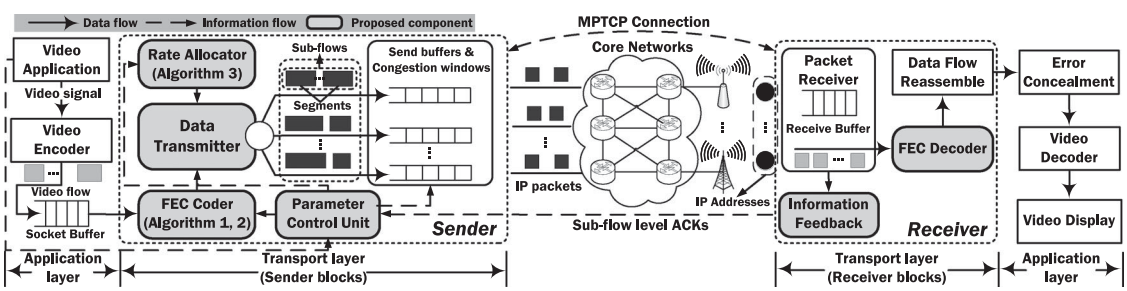

Fig. 2. System overview of the proposed ADMIT (quAlity-Driven Multipath TCP) scheme.

adjustment algorithms are implemented at the FEC coder. The flow rate allocation algorithm (Algorithm 3) is implemented at the rate allocator. The input parameters for the FEC coder include the communication path status (RTT_p, μ_p, π_p^B), delay constraint T, and FEC adaptation step size $\Delta\Theta, \Delta S$ (for redundancy and packet size). The parameters passed onto the Rate allocator include the communication path status (RTT_p, μ_p, π_p^B), delay constraint T, and threshold limit value (TLV). The role of the Parameter Control Unit is to collect the control parameters (delay constraint T, FEC adaption parameter), communication path status (round trip time, packet loss rate and available bandwidth) and output the decision parameters for the scheduling algorithms 1-3. The data transmitter is responsible for assigning the FEC packets onto different communication paths according to the rate allocation vector. This process can be implemented by the packet scheduling function in MPTCP [12], which associates segments sent on different sub-flows. For each decision epoch, the video frames are coded into the FEC packets and dispatched onto different communication paths at the data transmitter.

Algorithm 1. FEC Redundancy Adaption

Require: $\{RTT_p, \mu_p, \pi_p^B, m_p\}_{p\in\mathcal{P}}$, T, $\Delta\Theta = 0.5\%$; // m_p-consecutive losses over path p
Ensure: The FEC redundancy value Θ;
1: $\overline{RTT}_p \Leftarrow \frac{31}{32}\times\overline{RTT}_p + \frac{1}{32}\times RTT_p$, $\sigma_{RTT_p} \Leftarrow \frac{15}{16}\times\sigma_{RTT_p} + \frac{1}{16}\times|RTT_p - \overline{RTT}_p|$;
2: $\mathsf{ConI} \Leftarrow (m_p == 1)\,\&\&\,(RTT_p < \overline{RTT}_p - \sigma_{RTT_p})$, $\mathsf{ConII} \Leftarrow (m_p == 2)\,\&\&\,(RTT_p < \overline{RTT}_p - \sigma_{RTT_p}/2)$, $\mathsf{ConIII} \Leftarrow (m_p == 3)\,\&\&\,(RTT_p < \overline{RTT}_p)$, $\mathsf{ConIV} \Leftarrow (m_p > 3)\,\&\&\,(RTT_p < \overline{RTT}_p - \sigma_{RTT_p}/2)$;
3: **if** $(\mathsf{ConI}||\mathsf{ConII}||\mathsf{ConIII}||\mathsf{ConIV} == \mathrm{True})$ **then**
4: Thresh $\Leftarrow 1$; // random packet losses
5: **else**
6: **if** $RTT_p > \overline{RTT}_P + \frac{\sigma_{RTT_p}}{2}$ **then**
7: Thresh $\Leftarrow 0.6$; // congested status
8: **end if**
9: Thresh $\Leftarrow 0.8$; // mildly congested status
10: **end if**
11: $C_p \Leftarrow \frac{\max\{R_p,(n_p\cdot S)/\mathrm{T}\}\cdot(1+\Theta)}{\mu_p}$, $\Theta \Leftarrow \frac{\sum_{p\in\mathcal{P}}\pi_p^B}{P}$;
12: **while** $\{\max\{R_p, \frac{n_p\cdot S}{\mathrm{T}}\}\cdot(1+\Theta) < \mu_p\cdot(1-\pi_p^B)\,\&\&\,C_p <$ Thresh$\}$ **do**
13: $\Theta \Leftarrow \Theta + \Delta\Theta$;
14: Update the approximate function $\varphi(\Theta)$;
15: $U_p(\Theta, S) \Leftarrow \frac{\mu_p\cdot[1-\pi_p^{\mathrm{t}}-(1-\pi_p^{\mathrm{t}})\cdot\pi_p^{\mathrm{o}}]}{\max\{R_p,(n\cdot S)/\mathrm{T}\}\cdot(1+\Theta)}$, $\Delta U_p(\Delta\Theta) \Leftarrow \frac{\varphi(\Theta+\Delta\Theta)-\varphi(\Theta)}{\Delta\Theta/\mu_p}$;
16: **Procedure**: $S \Leftarrow$ PacketSizeAdaption (Θ); // Algorithm 2
17: **end while**
18: **return** $\Theta \Leftarrow \arg\max\{\sum_{p\in\mathcal{P}} U_p(\Theta, S)\}$;

At the receiver side, the information feedback unit is responsible for periodically sending back the channel status information (round trip time, available bandwidth and packet loss rate), which is involved in the scheduling algorithms at the sender side. ADMIT employs the same connection and sub-flow level acknowledgements (ACKs) mechanisms specified in the baseline MPTCP [12]. Due to the path asymmetry in heterogeneous wireless networks, the packets may arrive at the destination out-of-order. These packets will be reordered by the Data Flow Reassemble block (i.e., the MPTCP reordering buffer) to reconstruct the original video traffic for the decoding process. To ensure the in-order data delivery, the arrival packets are temporarily stored in a connection-level receive buffer until being read by the video application. A larger receive buffer can tolerate higher level of packet reordering and the size should be able to store all data until the missing segment is successfully retransmitted [12]. The basic frame-copy error concealment is implemented at the application layer of the receiver side to mitigate the playback disruptions.

Algorithm 2. FEC Packet size Adaption

Require: $RTT_p, \mu_p, \pi_p^B, R, \Delta S, S = MSS$;
Ensure: The FEC packet size S;
1: **while** $\{(S > 0)\,\&\&\,[\mathbb{E}(d_p^{\mathrm{E}}) < \mathrm{T}]\}$ **do**
2: $S' \Leftarrow S$, $S \Leftarrow S - \Delta S$, $n \Leftarrow \lceil(1+\Theta)\cdot k\rceil$;
3: $n_p \Leftarrow \frac{R_p}{\sum_{i=1}^{P} R_i}\cdot n$, $\pi_p^{\mathrm{o}} \Leftarrow \exp\left[-\frac{\mathrm{T}}{\mathbb{E}(d_p^{\mathrm{T}})+\mathbb{E}(d_p^{\mathrm{N}})}\right]$;
4: $\pi_p^{\mathrm{t}} \Leftarrow \frac{1}{n_p}\cdot\sum_{\forall c_p}\{\mathcal{L}(c_p)\cdot\pi_p^{c_p^1}\cdot\prod_{i=1}^{n-1}[\mathrm{F}_p^{\langle c_p^i, c_p^{(i+1)}\rangle}(\theta_p)]\}$;
5: $\Pi_p(\Theta, S) \Leftarrow \pi_p^t(n,k,S) + \left[1-\pi_p^t(n,k,S)\right]\cdot\pi_o(n,k,S)$;
6: $\Pi(\Theta, S) \Leftarrow$ Equation (7), $U(\Theta, S) \Leftarrow \sum_{p\in\mathcal{P}} U_p(\Theta, S)$;
7: **if** $\{\Pi(\Theta, S) > \Pi(\Theta, S')||U(\Theta, S) < U(\Theta, S')\}$ **then**
8: **break**;
9: **end if**
10: **end while**
11: **return** $S \Leftarrow \arg\min\left|\frac{\sum_{p\in\mathcal{P}} R_p\cdot\Pi_p(\Theta,S)}{\sum_{p\in\mathcal{P}} R_p} - \frac{n-k}{n}\right|$;

Algorithm 3. Reliability-Aware Flow Rate Allocation

Require: $\{RTT_p, \mu_p, \pi_p\}_{p\in\mathcal{P}}$, T, Δ, TLV $= 1.25$;
Ensure: $\{\mathcal{R} = \{R_p\}_{p\in\mathcal{P}}, n, k\}$;
1: **for** each path p in $\mathcal{P}$ **do**
2: $\mathsf{E}_p \Leftarrow \frac{1-\pi_p^B}{RTT_p}\cdot\exp\left\{\frac{\exp[1-(1-\Lambda_p)/10]-1}{\max\{R_p,(n_p\cdot S)/\mathrm{T}\}\cdot(1+R)}\right\}$;
3: $R_p \Leftarrow (R\cdot\mathsf{E}_p)/\sum_{p\in\mathcal{P}}\mathsf{E}_p$;
4: **if** $\mathsf{D}(p\in\mathcal{P}) > \mathsf{D}(p\notin\mathcal{P})$ **then**
5: $R_p \Leftarrow 0$, continue // End this loop if path p increases D;
6: **end if**
7: $\mathsf{L}_p \Leftarrow \frac{\mu_p\cdot(1-\pi_p^B)-\max\left\{R_p, \frac{n_p\cdot S}{\mathrm{T}}\right\}\cdot(1+R)}{\left\{\sum_{i=1}^{P}\mu_i\cdot(1-\pi_i^B)-\sum_{i=1}^{P}\max\left\{R_i, \frac{n_i\cdot S}{\mathrm{T}}\right\}\cdot(1+R)\right\}/P}$;
8: Estimate the FEC parameters (n,k) with Algorithm 1;
9: $\Delta R_p \Leftarrow \Delta R_p/U_p$, $R_p \Leftarrow R_p + \Delta R_p$;
10: Update the approximate function $\varphi(R_p)$;
11: **if** $\mathsf{L}_p \le$ TLV **then**
12: $R_p \Leftarrow R_p + \Delta R_p$ // Intra-path allocation;
13: Update the available resources of path p;
14: **else**
15: $\Delta\Pi \Leftarrow \sum_{p\in\mathcal{P}}\frac{\Pi_p(R_p)-\Pi_p(R_p+\Delta R_p)}{\Delta R_p}$;
16: $p' \Leftarrow \arg\max\{\Delta\Pi\}$, subject to $p'\in\mathcal{P}\,\&\&\,p'\neq p$, $\Delta R_p + \Delta R_{p'} = 0$ // Inter-path allocation;
17: **if** $\Delta\Pi > 0$ **then**
18: $R_p \Leftarrow R_p + \Delta R_p$;
19: Update the reliability parameters of path p and p';
20: **end if**
21: **end if**
22: **end for**
23: $\{\mathcal{R}, n, k\} \Leftarrow \arg\min\left|\frac{\alpha}{\sum_{p\in\mathcal{P}} R_p - R_0} + \beta\cdot\frac{\sum_{p\in\mathcal{P}} R_p\cdot\Pi_p(R_p,n_p)}{\sum_{p\in\mathcal{P}} R_p}\right|$;

TABLE 2
Definitions of Basic Notations

Symbol	Definition
$\mathbb{P}, \mathbb{E}, \mathbb{I}$	probability, expectation value, indicator function.
$\mathcal{P}, p$	set of communication paths, a path element.
P	number of communication paths.
$\mathcal{R}, R_p$	flow rate allocation vector, an element.
T, Θ	delay constraint, FEC redundancy value.
RTT_p, μ_p	round trip time, available bandwidth of p.
D	end-to-end distortion.
$\mathsf{D}_{\mathrm{src}}, \mathsf{D}_{\mathrm{chl}}$	source, channel distortion.
G/B	Good/Bad state of p.
π_p^B, ρ_p	packet loss rate, available source rate of p.
Π, Π_p	effective packet loss rate, over p.
$\pi_p^{\mathrm{t}}, \pi_p^{\mathrm{o}}$	transmission, overdue loss rate over p.
ξ_p^G	state transition probability of p from B to G.
n, k	total number of FEC packets, source packets.
C_p, U_p	congestion-level, utility of path p.
$\mathsf{L}_p, \mathsf{E}_p$	load imbalance factor, reliability parameter of p.
d_p^{E}	end-to-end connection delay over path p.
$d_p^{\mathrm{T}}, d_p^{\mathrm{N}}$	TCP-level, network-level delay over path p.
$\mathrm{F}_p^{\langle i,j \rangle}(\theta_p)$	state transition probability of p from i to j in θ_p.
MSS, S	maximum segment size, FEC packet size.

The optimization problem of joint FEC coding adaption and multipath rate allocation involves the models of wireless access network [2], video quality [36], FEC coding [37], and end-to-end connection delay [20]. The aggregate throughput of a MPTCP connection is impacted by the end-to-end connection states of the available communication paths. For instance, if there is bandwidth shrink/packet losses on one communication path, the throughput fluctuations can be mitigated by assigning more traffic loads to another path with better quality. Thus, analyzing the connection state is important in the FEC coding adaption and flow rate allocation. For the sake of completeness and integration with the system framework, these models are also presented in this section. The basic notations used throughout this paper are listed in Table 2.

3.2 Model Description

3.2.1 Wireless Access Network Model

We consider a heterogeneous wireless environment integrating P access networks between communication terminals. The wireless access networks represent the communication paths in MPTCP, which include wired and wireless domains. Each communication path $p \in \mathcal{P}$ is an independent transport link and characterized with the following properties.

Property 1 (Round trip time RTT_p). *The elapsed time for a packet to be delivered to the destination plus the delay it takes for an acknowledgment of that packet to be received. Therefore, RTT_p consists of the packet transmission time and path propagation delay.*

Property 2 (Packet loss rate π_p^B). *The average percentage of data packets failed to arrive at the destination while travelling across the communication paths. These packet drops can be caused by the network congestion, wireless channel fading, external interference, etc.*

Property 3 (Available bandwidth μ_p). *The maximum transmission rate that the end-to-end communication path can provide to the video flow [38]. In HTTP/TCP video streaming systems, the available bandwidth can be estimated according to the observed TCP throughput. In this work, we use the confidence intervals (with the sample size of 5) to combine the historical estimated values [5].*

The above channel status information can be periodically estimated using end-to-end network measurement techniques [38]. In this work, we employ the multipath status estimation model developed in [5] to accurately sense the path quality. We model the burst packet losses over end-to-end communication path as a continuous time stochastic process based on the Gilbert loss model [39]. The state $\mathcal{X}_p(t)$ of path p at time t assumes one of two values: G (Good) or B (Bad). We assume the packet loss rate to be zero in the 'Good' state [40]. If a packet is sent at time t with $\mathcal{X}_p(t) = G$, then the packet can be successful delivered. Otherwise, when $\mathcal{X}_p(t) = B$, then the packet is lost. We use the notations π_p^G and π_p^B to denote the stationary probabilities that the communication path is good or bad. Let ξ_p^B and ξ_p^G represent the transition probability from G to B and B to G, respectively. In this work, we adopt two system-dependent parameters to specify the continuous time Markov chain packet loss model: (1) the average loss rate π_p^B, and (2) the average loss burst length $1/\xi_p^G$. Then, we can have $\pi_p^B = \xi_p^B/(\xi_p^B + \xi_p^G)$ and $\pi_p^G = \xi_p^G/(\xi_p^B + \xi_p^G)$.

Remark. An important problem in FEC coding redundancy adaption is to *distinguish the congestion losses from random losses* [41]. In the congested network status, the available bandwidth will shrink and more data packets encounter channel losses. If we try to add more FEC redundant packets, it will increase the network congestion level and cause further packet losses. This *vicious congestion circle* is already observed in [41], [42]. In the literatures, many schemes have been proposed for the packet loss differentiation. For instance, the TCP Veno [43] identifies the congestion losses by estimating the backlogged packets at bottleneck link. In this study, we employ the ZigZag scheme [44] for the end-to-end packet loss differentiation based on the number of consecutive losses (m_p), average RTT_p ($\overline{RTT}_p$) and the standard deviation (σ_{RTT_p}). The ZigZag scheme is selected with regard to the fairness in bandwidth sharing, TCP-friendliness, and low misclassification rate [44].

3.2.2 Video Quality Model

To characterize the real-time streaming video quality, we employ a generic end-to-end video distortion model developed in [36]. The user-perceived quality in video streaming environment is impacted by the end-to-end distortion (D). Specifically, D is the sum of two major categories of distortion: source distortion ($\mathsf{D}_{\mathrm{src}}$) and channel distortion ($\mathsf{D}_{\mathrm{chl}}$), i.e.,

$$\mathsf{D} = \mathsf{D}_{\mathrm{src}} + \mathsf{D}_{\mathrm{chl}}. \tag{1}$$

Specifically, the source distortion is mostly driven by the video content characteristics and encoding parameters.

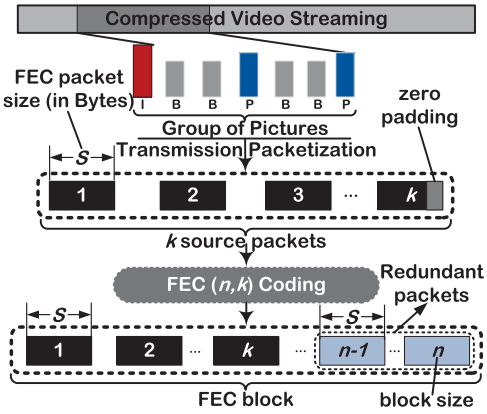

Fig. 3. Illustration of GoP-level systematic FEC coding process.

These parameters largely impact the efficiency of video codec (e.g., the larger distortion will be induced for a more complex video sequence under the same video encoding rate). As the source coding parameters are out of the control scope of ADMIT, we focus on the channel distortion, which is caused by the *effective packet loss rate* (Π) defined as follows.

Definition 1 (Effective packet loss rate Π). *The ratio of lost video data after the FEC recovery process. This loss probability includes both the channel errors/losses and expired packet arrivals.*

D_{chl} is roughly proportional to the number of video frames that cannot be decoded. In particular, the end-to-end distortion can be expressed (in units of Mean Squared Error, MSE) with the following equation [36], [45]:

$$\mathsf{D} = \underbrace{\frac{\alpha}{R - R_0}}_{\mathsf{D}_{\text{src}}} + \underbrace{\beta \cdot \Pi}_{\mathsf{D}_{\text{chl}}}, \tag{2}$$

in which R denotes the video encoding rate and α, R_0, β are parameters depending on specific video codec and sequence. These parameters can be online estimated by using trial encodings at the sender side [2], [45]. To allow fast adaptation of the transmission scheduling to abrupt changes in the video content, these parameters can be updated for each group of pictures (GoP).

3.2.3 Systematic FEC Model

We use the systematic Reed-Solomon (RS) [37] code for video data protection against wireless channel losses. The main motivation to choose the RS code over the popular fountain code is the stringent delay constraint. As shown in Fig. 3, a FEC block of n data packets contains k source packets and $(n-k)$ redundant packets. The receiver is able to reconstruct all the k source packets if any k packets of the FEC block are correctly received. In the FEC(n,k) coding, $(n-k)$ redundant data packets are introduced for every k source packets to make up a codeword. If the number of received packet is less than k, the received packets can still be used for the decoding process due to the systematic nature of the FEC code.

In this work, we implement the GoP-level FEC coding for the data protection. In each FEC coding phase, the video frames in each GoP are made into k source packets. For the last source packet, some zero bytes are often padded to keep the same size with other packets. The FEC packet size (S) also affects the tradeoff between loss recoverability and end-to-end delay in the presence of burst losses. With a smaller FEC packet size, the value of n (FEC block size) will become larger and there is higher possibility for the receiver to recover the lost packets. However, a larger FEC block size also delays the FEC decoding because: 1) more FEC packets will result in higher protocol overhead and this induces larger end-to-end delay; 2) the probability of packet reordering will also increase and the additional recovery time degrades the delay performance.

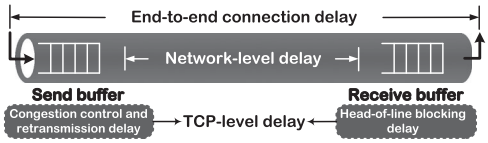

Fig. 4. Delay performance components.

3.2.4 End-to-End Connection Delay Model

In this work, we employ the TCP delay performance model in [20] to analyze the end-to-end connection delay (d_p^{E}) for each communication path in MPTCP. d_p^{E} includes two main components (shown in Fig. 4): 1) network-level delay (d_p^{N}); 2) TCP-level delay (d_p^{T}), i.e.,

$$d_p^{\text{E}} = d_p^{\text{N}} + d_p^{\text{T}}. \tag{3}$$

The TCP-level delay is dependent on the end-to-end connection state, and this state is determined by the congestion control phase [20]. Specifically, the TCP-level delay includes the congestion control and head-of-line blocking time. The head-of-line blocking delay is caused by the TCP receive buffering (the purpose of the receive buffer is to hold out-of-order packets while a loss is being detected). The network-level latency consists of the packet transmission and path propagation delays. We employ the Markov chain model developed in [20] to analyze the TCP-level delay. According to the Equation (3) in [20], the steady-state TCP delay distribution is modeled as follows

$$\mathbb{P}(d_p^{\text{T}} = d) = \frac{\sum_{s\in\Omega} \epsilon_s \cdot \sum_{s'\in\Omega} \text{P}_{\langle s,s'\rangle} \cdot \sum_{i=1}^{n_{\langle s,s'\rangle}} \mathbb{I}_{d^i_{\langle s,s'\rangle}=d}}{\sum_{s\in\Omega} \epsilon_s \cdot \sum_{s'\in\Omega} \left(\text{P}_{\langle s,s'\rangle} \cdot n_{\langle s,s'\rangle}\right)}, \tag{4}$$

in which $\mathbb{I}$ represents the indicator function and ϵ_s denotes the steady-state distribution of the Markov chain. $n_{\langle s,s'\rangle}$ represents the number of packets to be sent from state s to s' and $\text{P}_{\langle s,s'\rangle}$ denotes the state transition probability. The set (Ω) of the states (s) is defined as follows [20]

$$\Omega = \{\text{Application Limited (AL)}, \text{Congestion Avoidance (CA)}, \text{Slow Start (SS)}, \text{Fast Recovery (FR)}, \text{Timeout (TO)}\}.$$

The notation $d^i_{\langle s,s'\rangle}$ denotes the TCP delay of the ith packet sent in a transition from state s to s' and is expressed as follows

$$d^i_{\langle s,s'\rangle} = \begin{cases} b_p/R_p + RTT_p + (3+i)/f_p, & \text{if } s' \in \text{FR}, \\ b_p/R_p, & \text{otherwise}, \end{cases} \tag{5}$$

where b_p denotes the backlogged packets and f_p represents the load in packets per second. The packet backlogging can also be caused by the Nagle's algorithm [46] that complements the TCP to limit the transmission of small segments. However, this algorithm is disabled in many delay-constrained multimedia applications to reduce the retransmission delay [20] and we also follow this practice in this work. The backlog evolution for two consecutive states is modeled by

$$b_p = \begin{cases} \max\{0, b_p + R_p \cdot t_{\langle s,s'\rangle} - S\}, \text{if } s == \text{AL} \,\&\&\, s' == \text{AL}, \\ \max\{0, b_p + R_p \cdot t_{\langle s,s'\rangle} - \omega_p \cdot MSS\}, \text{ if } s' \in \{\text{CA}, \text{SS}\}, \\ \max\{0, b_p + R_p \cdot t_{\langle s,s'\rangle} - (\omega_p + 3) \cdot MSS\}, \text{ if } s' == \text{FR}, \\ \max\{0, b_p + R_p \cdot t_{\langle s,s'\rangle}\}, \text{ if} s' == \text{TO}, \end{cases}$$

where $t_{\langle s,s'\rangle}$ denotes the time interval from the state s to s' and the congestion window size ω_p can be estimated with the formula $\omega_p = \mu_p \cdot RTT_p$. The number of packets ($n_{\langle s,s'\rangle}$) sent from s to s' in Equation (4) is expressed as follows

$$n_{\langle s,s'\rangle} = \begin{cases} 1, \text{if } s == \text{AL} \,\&\&\, s' == \text{AL}, \\ \lfloor \min\{b_p, \omega_p \cdot MSS\}/S \rfloor, \text{if } s' \in \{\text{CA}, \text{SS}\}, \\ \lfloor \min\{b_p, (\omega_p + 3) \cdot MSS\}/S \rfloor, \text{if } s' == \text{FR}, \\ 0, \text{if } s' == \text{TO}, \end{cases}$$

The expectation value of the TCP-level delay $\mathbb{E}[d_p^{\text{T}}]$ can be calculated according to the delay distribution and the above model parameters.

The network-level delay d_p^{N} for a single FEC packet can be estimated using the following equation

$$d_p^{\text{N}} = \frac{\mu_p \cdot (1 - \pi_p^B)}{S} + \frac{\rho_p}{\mu_p - R_p}, \tag{6}$$

where $\mu_p \cdot (1 - \pi_p^B)$ represents the "loss-free" bandwidth and S denotes the FEC packet size. The 'loss-free' bandwidth is a good indicator of available capacity for end-to-end data transport over lossy paths [26]. ρ_p denotes the available source rate and is estimated using the latest historical values of path status information in conjunction with the assigned video traffic rate [2], [5], [45]

$$\rho_p = \frac{(\overline{\mu}_p - R_p) \cdot RTT_p}{2},$$

in which $\overline{\mu}_p$ denotes the average value of the latest measured (with the sample size of 5) available bandwidth.

3.2.5 Effective Packet Loss Rate

As explained in **Definition** 1, the effective packet loss rate is the combined probability of the transmission and overdue loss rates defined as follows.

Definition 2 (Transmission loss rate π_p^{t}). *The percentage of FEC packets that encounter channel losses or buffer overflows in packet switching networks.*

Definition 3 (Overdue loss rate π_p^{o}). *The probability of expired arrivals of FEC packets at the destination out of the delay constraint imposed by the real-time video application.*

If the effective packet loss rate Π is smaller than the tolerable loss rate $\frac{n-k}{n}$, the FEC coder is able to recover all the video frame data and the value of Π is zero. Otherwise, Π is estimated with $\frac{\sum_{p\in\mathcal{P}} R_p \cdot \Pi_p}{\sum_{p\in\mathcal{P}} R_p}$. With regard to the systematic FEC (n, k) coding process, the effective packet loss rate Π is expressed as follows

$$\Pi = \begin{cases} 0, & \text{if } \frac{\sum_{p\in\mathcal{P}} R_p \cdot \Pi_p}{\sum_{p\in\mathcal{P}} R_p} < \frac{n-k}{n}, \\ \frac{\sum_{p\in\mathcal{P}} R_p \cdot \Pi_p}{\sum_{p\in\mathcal{P}} R_p}, & \text{otherwise}, \end{cases} \tag{7}$$

in which Π_p denotes the effective packet loss rate over p. The overdue loss rate is imposed on the received video data after experiencing the channel losses and FEC recovery process. Therefore, the effective packet loss rate over path p can be expressed as

$$\Pi_p = \pi_p^{\text{t}} + (1 - \pi_p^{\text{t}}) \cdot \pi_p^{\text{o}}. \tag{8}$$

We decompose the analysis into two procedures. First, we provide theoretical derivations on the transmission loss rate based on Gilbert model and continuous time Markov chain.

Let c_p denote a n_p-tuple that represents a particular failure configuration during the transmission. The value of n_p is proportional to the rate allocation of p. If the ith packet in a FEC block is lost, then $c_p^i = B$, $1 \le i \le n_p$ and vice versa. By considering all the possible configurations of c_p, we can compute the transmission loss rate π_p^{t} as

$$\pi_p^{\text{t}} = \frac{1}{n_p} \sum_{\forall c_p} \mathcal{L}(c_p) \cdot \mathbb{P}(c_p), \tag{9}$$

where $\forall c_p$ indicates for all the possible combinations of c_p. $\mathcal{L}(c_p)$ represents the number of lost FEC packets for a given c_p. Specifically, $\mathcal{L}(c_p)$ is expressed as follows

$$\mathcal{L}(c_p) = \sum_{i=1}^{n_p} 1_{\{c_p^i = B\}}.$$

Let $\mathbb{P}(c_p)$ denote the probability of the path failure configuration in the transmission of the n_p packets. The derivation of $\mathbb{P}(c_p)$ with the continuous time Gilbert loss model is the product of the state transition probabilities. We use the notation $\text{F}_p^{\langle i,j\rangle}(\theta_p)$ to express the transition probability of path p from state i to j in time interval θ_p

$$\text{F}_p^{\langle i,j\rangle}(\theta_p) = \mathbb{P}[\mathcal{X}_p(\theta_p) = j | \mathcal{X}_p(0) = i]. \tag{10}$$

According to the property of continuous time Markov chain, we have the following state transition matrix:

$$\begin{bmatrix} \text{F}_p^{\langle G,G\rangle}(\theta_p) & \text{F}_p^{\langle G,B\rangle}(\theta_p) \\ \text{F}_p^{\langle B,G\rangle}(\theta_p) & \text{F}_p^{\langle B,B\rangle}(\theta_p) \end{bmatrix} = \begin{bmatrix} \pi_p^G + \pi_p^B \cdot \kappa_p & \pi_p^B - \pi_p^B \cdot \kappa_p \\ \pi_p^G - \pi_p^G \cdot \kappa_p & \pi_p^B + \pi_p^G \cdot \kappa_p \end{bmatrix},$$

in which $\kappa_p = \exp[-(\xi_p^B + \xi_p^G) \cdot \theta_p]$. In this study, we assume the intervals between the consecutive FEC packets are identical (i.e., evenly spread) to facilitate the analysis and packet scheduling. Now, the expression of $\mathbb{P}(c_p)$ can be obtained, e.g., for $n_p = 3$, $c_p^3 = B | c_p^2 = B | c_p^1 = G$ we have

$$\mathbb{P}[c_p^3 = B | c_p^2 = B | c_p^1 = G] = \pi_p^G \cdot \mathrm{F}_p^{\langle G,B\rangle}(\theta_p^1) \cdot \mathrm{F}_p^{\langle B,B\rangle}(\theta_p^2),$$

in which θ_p^i is the time interval between the ith and $(i+1)$th FEC packet. Therefore, $\mathbb{P}(c)$ can be computed as follows

$$\mathbb{P}(c_p) = \pi_p^{c_p^1} \cdot \prod_{i=1}^{n_p-1} \left[\mathrm{F}_p^{\left\langle c_p^i, c_p^{(i+1)} \right\rangle}(\theta_p) \right]. \tag{11}$$

Finally, after a sequence of algebraic manipulations, we have the transmission loss rate as

$$\pi_p^{\mathrm{t}} = \frac{1}{n_p} \cdot \sum_{\forall c_p} \left\{ \mathcal{L}(c_p) \cdot \pi_p^{c_p^1} \cdot \prod_{i=1}^{n_p-1} \left[\mathrm{F}_p^{\left\langle c_p^i, c_p^{(i+1)} \right\rangle}(\theta_p) \right] \right\}. \tag{12}$$

Now, we provide derivations on the overdue loss rate π_p^o, which is dependent on both the network characteristics and traffic arrival process. According to the delay statistics and latency distribution in existing studies on video streaming [45], [47], the end-to-end packet service time (queueing delay) can be modeled with exponential distribution in a capacity-limited communication network.

On the other side, it is also a challenging task to model the packet arrival process of real-time video streaming, as the traffic rate and packet size may be time-varying. Recent studies [45], [47], [48] reveal that the video traffic pattern follows the Markov arrival process. In this study, we consider each communication path as a queueing system with a single server. Therefore, we model the queueing delay with the $M/G/1$ model and the overdue loss probability of packets over the communication network is expressed as [5], [45], [47]

$$\pi_p^{\mathrm{o}} = \mathbb{P}\left[\mathbb{E}(d_p^{\mathrm{E}}) > \mathrm{T} \right] \approx \exp\left[-\frac{\mathrm{T}}{\mathbb{E}(d_p^{\mathrm{E}})} \right], \tag{13}$$

where $\mathbb{E}(d_p^{\mathrm{E}})$ denotes the expected value of end-to-end delay and can be obtained with Equations (3), (4) and (6). Therefore, the ratio of expired arrival FEC packets is calculated with the following equation

$$\pi_p^{\mathrm{o}} \approx \exp\left[-\frac{\mathrm{T}}{\mathbb{E}\left(d_p^{\mathrm{T}}\right) + \mathbb{E}\left(d_p^{\mathrm{N}}\right)} \right]. \tag{14}$$

Based on Equations (7), (8), (12) and (14), we can estimate the expectation value of Π.

3.3 Problem Statement

After introducing the mathematical models, the optimization problem can be stated as follows. Given the delay constraint T, communication path status $\{RTT_p, \pi_p^B, \mu_p\}_{p\in\mathcal{P}}$, find the rate allocation vector $\mathcal{R} = \{R_p\}_{p\in\mathcal{P}}$ and FEC coding parameters (n,k) to minimize the end-to-end distortion. Mathematically, this optimization can be formulated as

$$\begin{aligned} &\textbf{Determine the values of } n, k, \mathcal{R} = \{R_p\}_{p\in\mathcal{P}}, \\ &\textbf{to minimize } \mathsf{D} = \frac{\alpha}{\sum_{p\in\mathcal{P}} R_p - R_0} + \beta \cdot \Pi, \\ &\text{subject to} \begin{cases} \mathbb{E}(d_p^{\mathrm{N}}) + \mathbb{E}(d_p^{\mathrm{T}}) < \mathrm{T}, & \text{(16a)} \\ \max\left\{ \frac{R_p \cdot n}{n_p \cdot S} \right\} < \mu_p \cdot (1 - \pi_p^B) & \text{(16b)} \end{cases} \end{aligned} \tag{15}$$

where $\Pi =$ Equation (7),

$$\begin{aligned} \Pi_p &= \pi_p^{\mathrm{t}} + (1 - \pi_p^{\mathrm{t}}) \cdot \pi_p^{\mathrm{o}}, \\ \pi_p^{\mathrm{t}} &= \frac{1}{n_p} \cdot \sum_{\forall c_p} \left\{ \mathcal{L}(c_p) \cdot \pi_p^{c_1} \cdot \prod_{i=1}^{n-1} \left[\mathrm{F}_p^{\left\langle c_p^i, c_p^{(i+1)} \right\rangle}(\theta_p) \right] \right\}, \\ \pi_p^{\mathrm{o}} &= \exp\left[-\frac{\mathrm{T}}{\mathbb{E}(d_p^{\mathrm{T}}) + \mathbb{E}(d_p^{\mathrm{N}})} \right], \\ \mathbb{E}(d_p^{\mathrm{T}}) &= \text{Equation (4)}, \\ \mathbb{E}(d_p^{\mathrm{N}}) &= \frac{\mu_p \cdot (1 - \pi_p^B)}{n \cdot S} + \frac{\rho_p}{\mu_p - R_p}, \\ \rho_p &= \frac{(\overline{\mu}_p - R_p) \cdot RTT_p}{2}. \end{aligned}$$

As stated in condition (16a), the end-to-end connection delay is limited to be less than the delay constraint to prevent the palyback buffer starvation. In order to ensure the stable state of the communication system, (16b) regulates the total traffic rate (after adding the FEC redundant packets) should not exceed the available bandwidth with regard to the video traffic variation [49]. Note that the video encoding rate $R = \sum_{p\in\mathcal{P}} R_p$ is not a fixed parameter for constant bit-rate video streaming due to the bit rate variability [49]. Therefore, the actual bit rate is dynamically estimated with the division of video data size to the playout duration.

The joint optimization problem of rate allocation and FEC coding is NP-hard [50]. It is computationally prohibitive to directly solve this problem for the optimal solution. Therefore, we present a utility maximization based FEC coding and rate allocation framework to solve the optimization problem (15) with polynomial time complexity. The challenging issues to apply the utility maximization theory in optimization problem (15) can be summarized as: 1) In the context of multipath video communication, the throughput gains *cannot always* guarantee the video quality improvement with regard to the delay constraint [5]; 2) Under the path capacity constraint, it is also a critical problem to dynamically adapt the video flow rate and FEC redundancy level to achieve the optimal quality.

4 Solution Procedure of ADMIT

In this section, we describe the solution procedure of the proposed ADMIT solution in detail. The key decision blocks in the system design of ADMIT (i.e., the flow rate allocation and FEC coding adaption) are introduced to address the two critical issues in problem (15). Specifically, the FEC coding adaption is the execution procedure of the flow rate allocation. In each decision epoch (e.g., the duration of a GoP), the FEC coding scheme (Algorithm 1) is invoked in the rate approach algorithm to estimate the redundancy parameters (n,k).

We first introduce the FEC coding scheme that includes the redundancy level and packet size adaption. Then, we present the reliability model and rate allocation algorithm.

4.1 FEC Coding Adaption

It is a challenging issue to determine the FEC redundancy value with regard to the tradeoff between loss and delay performance. Fig. 5a depicts the variation of effective packet loss rate with the increase in FEC redundancy. The

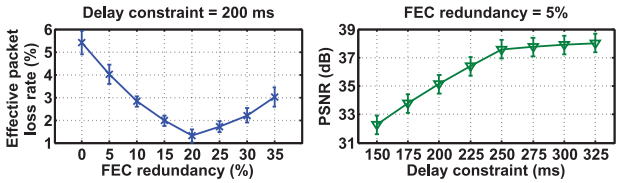

Fig. 5. Profile of tradeoff between: (a) effective packet loss rate and FEC redundancy level and (b) PSNR and delay constraint.

experimentation is performed with a single video flow (2.5 Mbps) over a Wi-Fi network. According to literature [51], the average packet loss rate of Wi-Fi networks mainly ranges from 2 to 6 percent. Therefore, the packet loss rate of the communication path is 6 percent in the emulations. The detailed experimental setup of network environments and video codec is specified in Section 5.1. With the imposed delay constraint of 200 ms, there is a sudden increase in the effective loss rate when the FEC coding redundancy is above 20 percent. The excessive FEC packets will significantly increase the end-to-end delay, which is not tolerable for the delay-stringent video applications (e.g., cloud gaming, video conferencing, etc.). To show the tradeoff between delay constraint and video PSNR, we also plot the relationship in Fig. 5b. It can be observed from the result that the increase in PSNR values is rapid for tight delay constraints but becomes slow in the relatively loose deadlines. In the following, we will introduce the FEC redundancy estimation algorithms for each coding phase.

4.1.1 FEC Redundancy Adaption

The FEC redundancy adaption is a critical problem in the decision process of multipath transfer since ADMIT intelligently sends FEC packets over different sub-flows. There is an inherent tradeoff between the FEC redundancy [$\Theta = (n-k)/k$] and delay performance due to the decoding deadline imposed by video applications [52]. By introducing more redundant packets, the receiver is able to recover from more serious transmission losses. However, a higher redundancy level also increases the end-to-end delay (overdue loss rate) and the possibility of network congestions.

In order to effectively take advantage of the available network resources to minimize the effective packet loss rate, we employ the utility maximization theory in the FEC redundancy adaption. Conventionally, the objective of the utility theory is to maximize the network throughput. Therefore, we introduce a congestion-level parameter C_p to indicate whether the network path is overloaded, and thus alleviate severe congestions. This parameter is motivated by the reliability model introduced in [53] and can be expressed as follows

$$C_p = \frac{\max\{R_p, (n_p \cdot S)/\mathrm{T}\} \cdot (1+\Theta)}{\mu_p}. \tag{17}$$

If the value of C_p is higher than a threshold value (Thresh) [30], the network is overloaded. In this work, we set the Thresh at three values (i.e., 1, 0.8 and 0.6) to limit the total traffic rate [38], [45], [54]. We set the value of Thresh to be: 1) 1 while the random packet loss occurs; 2) 0.8 in the mildly congested status; 3) 0.6 in the congested status [54].

To balance the tradeoff between the transmission and overdue loss rate, the piecewise linear approximation is employed to iteratively approach the FEC redundancy value and the motivation is justified in Theorem 1. The solution for optimization problem (15) to minimize the end-to-end distortion is in the convex union of many small hypercubes. Therefore, a optimal solution in the convex union can be obtained in the set of local solutions. We approximate the optimal solution by partitioning the interest region of each univariate function into an adequate number of non-overlapped small intervals. Assume that the initial FEC redundancy Θ is the averaged value of the latest redundancy levels. At the beginning of the video session, Θ is set to be the same value as the average packet loss rate $(\sum_{p\in\mathcal{P}} \pi_p^B)/P$. The utility level of path p is calculated with the following equation

$$U_p(\Theta, S) = \frac{\mu_p \cdot [1-\pi_p^{\mathrm{t}} - \left(1-\pi_p^{\mathrm{t}}\right)\cdot \pi_p^{\mathrm{o}}]}{\max\{R_p, (n\cdot S)/\mathrm{T}\}\cdot(1+\Theta)}. \tag{18}$$

Let $\Delta\Theta$ denote the redundancy increment at each iteration and $\Theta + \Delta\Theta$ represent the next transition. The utility variation of the redundancy adaption is expressed as [55]:

$$\Delta U_p(\Delta\Theta) = \frac{\varphi(\Theta+\Delta\Theta) - \varphi(\Theta)}{\Delta\Theta/\mu_p}, \tag{19}$$

in which $\varphi(\cdot)$ represents the approximate linear function for effective packet loss rate Π in the interval $[\Theta, \Theta+\Delta\Theta]$. In each iteration, the proposed redundancy adaption algorithm obtains the Θ that brings the highest utility, i.e.,

$$\Theta = \underset{\Theta}{\operatorname{argmax}}\left\{\sum_{p\in\mathcal{P}} U_p(\Theta, S)\right\},$$
$$\text{subject to}\begin{cases} \frac{\max\{R_p,(n_p\cdot S)/\mathrm{T}\}\cdot(1+\Theta)}{\mu_p} \le \mathrm{Thresh}, \\ \mathbb{E}[d_p^{\mathrm{N}}(\Theta,S)] + \mathbb{E}[d_p^{\mathrm{T}}(\Theta,S)] < \mathrm{T}, \\ \max\{R_p,(n_p\cdot S)/\mathrm{T}\}\cdot(1+\Theta) \le \mu_p\cdot(1-\pi_p^B). \end{cases}$$

The utility-maximization based FEC coding redundancy adaption scheme is outlined in Algorithm 1.

Theorem 1. *The piecewise linear approximation method based on utility theory is able to approach a optimal FEC redundancy value to minimize the effective packet loss rate.*

Proof. Please see the supplementary file, which can be found on the Computer Society Digital Library at http://doi.ieeecomputersociety.org/10.1109/TMC.2015.2497238. □

Proposition 1. *Algorithm 1 is a polynomial time approximation scheme for FEC coding parameter (n,k) adaption with the complexity of $O(\frac{(P-\sum_{p\in\mathcal{P}}\pi_p^B)\cdot MSS}{P\cdot\Delta\Theta\cdot\Delta S})$.*

Proof. In the worst case, the total number of iterations in the while loop of Algorithm 1 is $(P-\sum_{p\in\mathcal{P}}\pi_p^B)/(P\cdot\Delta\Theta)$. The time complexity of Algorithm 2 to approach the optimal FEC packet size is $\frac{MSS}{\Delta S}$. Consequently, the time complexity of Algorithm 1 is $O(\frac{P-\sum_{p\in\mathcal{P}}\pi_p^B}{P\cdot\Delta\Theta}\cdot\frac{MSS}{\Delta S})$. □

4.1.2 Packet Size Adaption

The FEC packet size also affects the tradeoff between loss recoverability and end-to-end delay. With a small packet size, the TCP-level delay can be reduced during the slow start process [20]. Furthermore, the FEC block will be more resilient to burst packet losses since the block size enlarges. On the other side, a larger FEC block size also delays the recovery process and increases the network overhead caused by adding packet headers. The FEC packet size adaption algorithm would interfere with the Nagle algorithm [46], which is disabled following the TCP setting in reference [20] to reduce retransmission delay.

To balance the tradeoff between delay performance and FEC recoverability, we propose a fast search algorithm to approach the optimal FEC packet size. Given the FEC redundancy value, *ADMIT seeks to use the minimal FEC packet size* that minimizes the difference between effective packet loss rate and tolerable loss rate $[(n-k)/k]$, i.e.,

$$S = \arg\min \left| \frac{\sum_{p\in\mathcal{P}} R_p \cdot \Pi_p(\Theta, S)}{\sum_{p\in\mathcal{P}} R_p} - \frac{n-k}{n} \right|.$$

To guarantee the network overhead will not degrade the overall system utility, the search will terminate if the utility level is lower than the last cycle. The detailed computation for the impact of the network overhead on the system utility is omitted here. Algorithm 2 presents the outline of the FEC packet size adaption. The search algorithm will terminate if the imposed constraints are violated or network resources are exhausted.

Remark. A larger packet size indicates a smaller FEC block size (n), which results in the less resilience to burst losses and lower accuracy of the packet loss rate estimation (due to the smaller number of samples in each estimation cycle). Therefore, a larger FEC packet size may also degrade the efficiency of redundancy adaption. ADMIT ensures the FEC packet size does not exceed the MSS so that the packet will not be fragmented at the network layer.

4.2 Reliability-Aware Flow Rate Allocation

In this section, we first introduce the reliability model for each communication path. Then, we present the reliability-aware rate allocation algorithm to minimize the end-to-end distortion while balancing the video data over different sub-flows to minimize the risk of sending all data from one GoP over the same path.

4.2.1 Reliability Model

This model is motivated by the availability model developed in [53] and the definition is presented as follows

Definition 4 (Path reliability E_p). *The capability of a communication path to successfully deliver real-time traffic and the mathematical expression is as follows*

$$\mathsf{E}_p = \frac{\mu_p \cdot (1-\pi_p^B)}{RTT_p} \cdot \exp\left\{ \frac{\exp\left[1-(1-\Lambda_p)/10\right]-1}{\max\{R_p, (n_p \cdot S)/\mathrm{T}\} \cdot (1+\Theta)} \right\}, \tag{20}$$

in which the numerator $\exp\left[1-(1-\Lambda_p)/10\right]-1$ *denotes the probability that path* p *is available and* Λ_p *represents the resource availability of the communication path. In this work,* Λ_p *is estimated with latest values of video traffic rate to available bandwidth.*

Equation (20) indicates the reliability of p is: 1) directly proportional to the available bandwidth μ_p; 2) inversely proportional to the assigned packet loss rate π_p^B, and round trip time RTT_p.

Now, we calculate the reliability E exhibited by the video transmission system over heterogeneous wireless networks. The system's reliability is expressed by Equation (21) and this metric denotes the overall transport capability.

$$\begin{aligned} \mathsf{E} &= \sum_{p\in\mathcal{P}} \left(\frac{R_p}{\sum_{i=1}^{P} R_i} \cdot \mathsf{E}_p \right), \\ &= \sum_{p\in\mathcal{P}} \left\{ \frac{R_p \cdot (1-\pi_p^B)}{RTT_p \cdot \sum_{i=1}^{P} R_i} \cdot \exp\left\{ \frac{\exp\left[1-(1-\Lambda_p)/10\right]-1}{\max\{R_p, (n_p \cdot S)/\mathrm{T}\} \cdot (1+\Theta)} \right\} \right\}. \end{aligned} \tag{21}$$

The above equation indicates we should balance the load among different communication paths to improve resource availability, and thus enhance the system reliability.

4.2.2 Rate Allocation Algorithm

To minimize the end-to-end video distortion, the rate allocation mechanism is inclined to assign loads to the communication paths with higher reliability. The reliability level presented by a communication path is proportional to the resource availability. However, such policy is extremely likely to induce load imbalance and link congestion because more traffic loads will be assigned to the paths with higher bandwidth and lower delay. The path asymmetry in heterogeneous wireless networks may also significantly increase the head-of-line blocking delay of specific communication paths. This is because more traffic loads are inclined to be assigned to the paths with higher quality. To alleviate severe load imbalance problems, we introduce a load imbalance parameter L_p to indicate whether path p is overloaded and it can be expressed as [5]

$$\mathsf{L}_p = \frac{\mu_p \cdot (1-\pi_p^B) - \max\left\{ R_p, \frac{n_p \cdot S}{\mathrm{T}} \right\} \cdot (1+\Theta)}{\sum_{i=1}^{P} \left\{ \mu_i \cdot (1-\pi_i^B) - \max\left\{ R_i, \frac{n_i \cdot S}{\mathrm{T}} \right\} \cdot (1+\Theta) \right\} / P}.$$

This parameter is motivated by the principle of balancing load in MPTCP congestion control [12], [24]. When the value of L_p is obviously higher than a threshold limit value [5], [47], path p is overloaded. We assume the initial rate allocation for each path is proportional to the reliability value, i.e., $R_p = (R \cdot \mathsf{E}_p)/\sum_{p\in\mathcal{P}} \mathsf{E}_p$. Let ΔR_p denote the rate variation over path p at each iteration and $R_p + \Delta R_p$ represent the transition of the next allocation. The variation in effective packet loss rate Π (of all the communication paths) resulted from the rate transitions can be expressed as:

$$\Delta\Pi = \sum_{p\in\mathcal{P}} \frac{\Pi_p(R_p) - \Pi_p(R_p + \Delta R_p)}{\Delta R_p}, \tag{22}$$

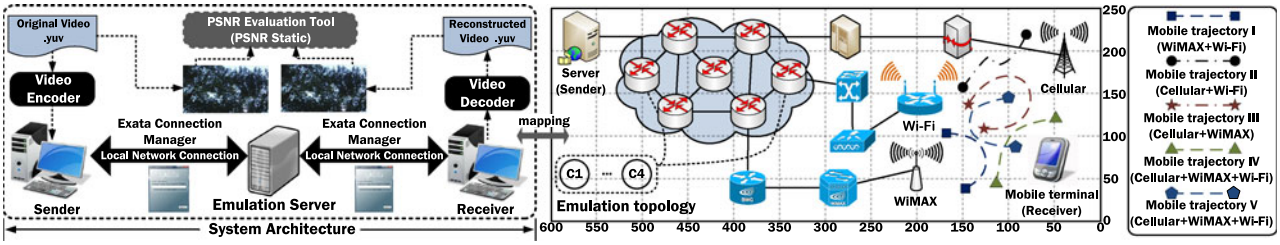

Fig. 6. System architecture and emulation topology for performance evaluation.

In each iteration, the proposed rate allocation algorithm obtains the rate allocation and FEC parameters that minimize the end-to-end distortion D, i.e.,

$$\begin{aligned}&\left\{\mathcal{R}=\{R_p\}_{p\in\mathcal{P}}, n, k\right\}\\&=\arg\min\left|\frac{\alpha}{\sum_{p\in\mathcal{P}}R_p-R_0}+\beta\cdot\frac{\sum_{p\in\mathcal{P}}R_p\cdot\Pi_p(R_p,n_p)}{\sum_{p\in\mathcal{P}}R_p}\right|,\\&\text{subject to maximize } \mathsf{E}=\sum_{p\in\mathcal{P}}\left[\frac{R_p}{\sum_{i=1}^{P}R_i}\cdot\mathsf{E}_p(R_p,n_p)\right].\end{aligned}\quad(23)$$

As the initial rate allocation vector cannot guarantee the minimal or near-minimal end-to-end distortion, we propose to use the intra and inter path rate allocation procedure to improve the video quality. The proposed algorithm exploits the network resources available in heterogeneous wireless networks in an iterative manner. Once the network resources of path p are exhausted, the algorithm will seek a different path which can release the required resources for the video flow. This operation will be performed until the end-to-end video distortion D cannot be further reduced or the available network resources are depleted. Algorithm 3 presents the sketch of the reliability-aware flow rate allocation scheme. The scheduler to distribute the load among the available paths in the MPTCP layer can be implemented in the Linux kernel. Specifically, the rate allocation vector $\mathcal{R}=\{R_p\}_{p\in\mathcal{P}}$ should be involved in the decision process of MPTCP packet scheduling function [10] when associating segments sent on different sub-flows.

In this algorithm, the intra-path allocation process always attempts to increase the systems utility by assigning some resources in path p. If the available resources are not adequate, this procedure will find a new flow that can release enough resources by allocating parts of its assigned rate through another path. For the proposed rate allocation algorithm, we can have the following two propositions.

Proposition 2. *The worst-case time complexity of Algorithm 3 is* $O(\frac{(P-\sum_{p\in\mathcal{P}}\pi_p^B)\cdot MSS}{\Delta\Theta\cdot\Delta S})$, *in which* P *denotes the number of communication paths.* $\Delta\Theta$ *and* ΔS *denote the steps of FEC redundancy and packet size adaption, respectively.*

Proof. There are P iterations in the *for* each loop (i.e., for each $p\in\mathcal{P}$) of Algorithm 1 since the total number of elements in the set of paths $\mathcal{P}$ is P. In each iteration, Algorithm 2 is invoked to estimate the FEC coding parameter and its time complexity is $O([(P-\sum_{p\in\mathcal{P}}\pi_p^B)\cdot MSS]/(P\cdot\Delta\Theta\cdot\Delta S))$ (see Proposition 1). Therefore, the worst-case time complexity of Algorithm 3 is $O(\frac{(P-\sum_{p\in\mathcal{P}}\pi_p^B)\cdot MSS}{\Delta\Theta\cdot\Delta S})$. □

Proposition 3. *If the maximal traffic rate of all sub-flows is less than or equal to the minimal available bandwidth of all communication paths, the inter-path allocation rate is zero.*

Proof. First, the maximal capacity requirement of all input flows is no more than the minimal available bandwidth of all communication paths. Second, the imposed traffic load does not exceed the aggregate capacity, i.e.,

$$\sum_{p\in\mathcal{P}}\left\{\max\{R_p,(n_p\cdot S)/\mathrm{T}\}\cdot(1+\Theta)\right\}\le\sum_{p\in\mathcal{P}}\mu_p\cdot(1-\pi_p^B).$$

Therefore, any single path is able to deliver a initially allocated sub-flow, i.e., $R_p\le\mu_p\cdot(1-\pi_p^B)$. The inter-path allocation procedure will not be executed. □

Remark. If the available bandwidth of all the communication paths $p\in\mathcal{P}$ is smaller than the video traffic rate R, the proposed flow rate allocation algorithm gracefully degrades to a load-balancing scheme. If any communication path p is overloaded, Step 11 in Algorithm 3 is invoked to balance the load across the heterogeneous access networks.

5 Performance Evaluation

In this section, we evaluate the efficacy of the proposed ADMIT via extensive semi-physical emulations in the network emulator Exata. The semi-physical emulations are different from the traditional trace-driven simulations (e.g., using NS-2 or OPNET). As shown in Fig. 6, the sender and receiver are connected to the emulation server through the Exata connection manager. The emulation setup and network environment are configured in the emulation server. The transmission ends in the emulation topology are mapped to the communication terminals in local networks to mimic real data transfer with high fidelity.

First, we describe the evaluation methodology that includes the emulation setup, performance metrics, reference schemes, and emulation scenario. Then, we present and discuss the emulation results in detail. The component-wise validation is shown at the end of this section.

5.1 Evaluation Methodology

5.1.1 Network Emulator

We use Exata 2.1 [56] as the network emulator. Exata is an advanced edition of QualNet [57] in which we can perform semi-physical emulations. In order to implement the real-video-streaming based emulations, we integrate the source code of JM (Joint Model) with Exata and develop an application layer protocol of "Video Transmission". The detailed descriptions of the development steps could be referred to

TABLE 3
Parameter Configurations of Wireless Networks

Cellular parameter	Value
Target SIR value	10 dB
Maximum power of BS	43 dB
Orthogonality factor	0.4
Common control channel power	33 dB
Total cell bandwidth	3.84 Mc/s
Background noise power	−106 dB
Inter/intra cell interference ratio	0.55
available bandwidth (trajectory)	1.2 (I-IV), 1.8 (V) Mbps
π_p^B, RTT_p	2%, 80 ms
WiMAX parameter	**Value**
System bandwidth	7 MHz
Number of carriers	256
Sampling factor	8/7
Average SNR	15 dB
Symbol duration	2,048
available bandwidth (trajectory)	1 (I-IV), 1.2 (V) Mbps
π_p^B, RTT_p	4%, 40 ms
WLAN parameter	**Value**
Average channel bit rate	3 Mbps
Slot time	10 μs
Maximum contention window	32
available bandwidth (trajectory)	0.8 (I-IV), 1 (V) Mbps
π_p^B, RTT_p	6%, 30 ms

Exata Programmer's Guide [56]. In the emulated network topology, the sender has one wired network interface and the mobile client has three wireless network interfaces, i.e., Cellular, WLAN and WiMAX. The parameter configurations of different wireless access networks (e.g., round trip time) are summarized in Table 3 [2], [5], [58].

As the MPTCP is not available in the transport-layer stack of the Exata emulator, we develop this transport protocol based on the TCP module and the C code from GitHub [59]. As depicted in the figure, each router is attached to one edge node, which is single-homed and introduces background traffic. Each of the edge nodes has four traffic generators producing cross traffic with a Pareto distribution. The packet sizes of background traffic are chosen to resemble the distribution measured from the Internet: 43 percent are large ($\geq$ 1,400 Bytes), 17 percent are medium [(144, 1,400) Bytes], and 40 percent are small ($\leq$ 144 Bytes) [60]. The aggregate cross traffic loads imposed on the available network paths are similar and vary randomly between $20 - 40$ percent of the bottleneck links' bandwidth. The data distribution interval is 250 ms (the duration of a GoP). The packet interleaving level (θ_p) is 2 ms for each communication path. The threshold limit value for L_p is set to be 1.25 [5], [47] in the emulations.

5.1.2 Video Codec

The reference software JM (Joint Model) 18.2 [61] for H.264/AVC is adopted as the video encoder. The generated video streaming is encoded at 30 frames per second and a GoP consists of 15 frames. The GoP structure is IPP...P. The test video sequences are *blue sky*, *mobcal*, *park joy*, *and river bed* in high definition (HD) content. These test sequences feature different patterns of temporal motion and spatial characteristics that reflected in their corresponding video quality versus encoding rates. We concatenate the video sequences to be 15,000 frame-long (500 seconds) in order to obtain statistically meaningful results. The delay constraint (T) for each GoP is set to be 500 ms to prevent playback buffer starvation. The streaming video is encoded at the source rates of 1.8, 2, 2.2, 3, and 4 Mbps for the Trajectory I to V.

5.1.3 Reference Schemes

- GreenBag [25]. This scheme includes the components of medium load balancing with recovery, segment management and energy-aware link mode control to stream real-time video over multiple TCP connections.
- FMTCP [21]. The fountain code based Multipath TCP (FMTCP) scheme exploits the random nature of fountain code to flexibly transmit encoded symbols over available communication paths. The data allocation is based on the expected arriving time and decoding demand.
- MPLOT [26]. This transport-layer protocol achieves transmission reliability with a proposed HARQ (Hybrid Automatic Request) mechanism. The FEC redundancy is provided in hybrid proactive/reactive manner and the FEC packets are mapped to different communication paths based on estimated quality.
- MPTCP [12]. The *baseline* MPTCP scheme is also used as a reference scheme for performance comparison. The congestion control, buffer management and data retransmission algorithms are specified in [12].

The above reference schemes are selected due to the representativeness, protocol layer stack, and implementation issues. The RTT-based scheduler (i.e., the default scheduler in MPTCP) is used in the evaluation of MPTCP results. Besides, the Explicit Congestion Notification (ECN) is enabled in the emulations for MPLOT to achieve its full performance.

5.1.4 Performance Metrics

- Peak Signal-to-Noise Ratio [62] is the standard metric to measure objective video quality. This metric is expressed as a function of the MSE between the original and the reconstructed video frames. If a video frame is dropped during transmission or past the deadline, it is considered to be lost and will be concealed by copying the content from the previously received frame.
- The *end-to-end delay* of a video frame consists of the transmission delay and the holding time at both server and client side. It is counted from the generation time of a video frame to the time when it can be decoded.
- *Goodput* represents the amount of useful information data successfully delivered to the destination within the imposed deadline T.

5.1.5 Emulation Scenarios

We conduct the emulations in mobile scenarios along the trajectories indexed from I to V as shown in Fig. 6. These

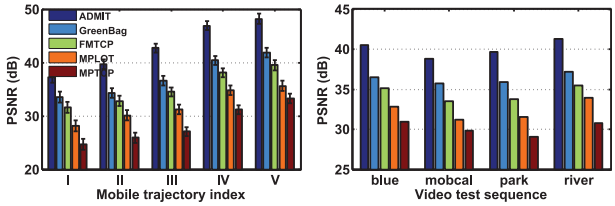

(a) different trajectories (b) different sequences

Fig. 7. Comparison of average PSNR results.

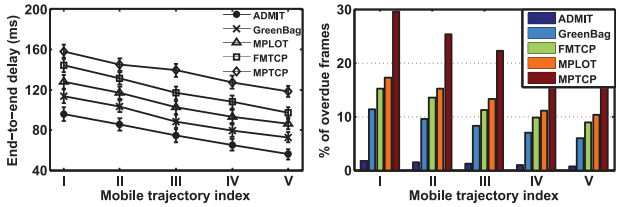

(a) end-to-end delay (b) overdue frames

Fig. 10. Comparison of delay performance.

mobile trajectories represent different access options and capacity constraints as specified in Fig. 6 and Table 3. The mobile terminal is set to move along these trajectories back and forth at the speed of 2 m/s.

In each transmission scenario, the emulation is repeated over 20 times obtain the average values with a 95 percent confidence interval. The microscopic results (time series analysis) are refined from a single run with finer granularity.

5.2 Evaluation Results

5.2.1 PSNR

Fig. 7a shows the average PSNR results obtained with the competing transport protocols along the mobile trajectories. ADMIT outperforms the GreenBag scheme due to the quality-driven optimization framework that incorporates the FEC coding and rate allocation. As the fountain code is not effective for real-time video applications with stringent delay constraint, FMTCP frequently induces large end-to-end packet delay and achieves lower quality than ADMIT. We can also observe the performance gaps become larger while moving along Trajectory II. The results indicate ADMIT is able to effectively overcome the path asymmetry in heterogeneous wireless networks as more access options are available in Trajectory II. The baseline MPTCP achieves the lowest PSNR values as it does not include the FEC scheme to overcome the channel losses. The mean PSNR values with regard to different test sequences in Trajectory III are shown in Fig. 7b. In order to have a close-up view of the microscopic results, the PSNR values for per video frame indexed from $[1{,}000, 2{,}000]$ are depicted in Fig. 8. Obviously, ADMIT achieves higher PSNR values with lower variations than the reference schemes.

To compare the subjective video quality of the competing schemes, the 618th received frames of Trajectory III (measured from the park joy sequence) are shown in Fig. 9. The frame received with ADMIT can be clearly seen while the images of the reference schemes are damaged to different levels.

5.2.2 End-to-End Delay

Fig. 10a shows the average end-to-end video frame delay for all the competing transport protocols. The results' pattern is almost the opposite to that shown in Fig. 7a. In real-time video applications, the media quality in terms of PSNR is generally inversely proportional to the end-to-end delay [28], [63]. This is because larger latency will incur more overdue packets and recent studies [28], [63] suggest the one-way delay should not exceed 150 ms to achieve excellent quality. In order to guarantee the acceptable quality, this delay is constrained to be less than 400 ms. Expectedly, ADMIT achieves the lowest end-to-end delay as it employs the RS code for data protection, and thus significantly reduces the number of unnecessary retransmissions. Of equal importance to the delay reduction, ADMIT takes into account the characteristics of MPTCP connection (e.g., fast recovery, congestion avoidance, slow start, etc.) in estimating the end-to-end connection delay. These important factors are not considered in the reference protocols. Thus, ADMIT provides higher estimation accuracy in the end-to-end delay than the reference schemes. Different from the rank in quality results, MPLOT outperforms the FMTCP in reducing the end-to-end delay. This is because the fountain code is of large block size, and thus results large additional delay. Fig. 10b plots the ratio of video frames past decoding deadline to compare the playback fluency achieved with different transmission schemes. FMTCP guarantees more video frames deliver within the delay constraint because it

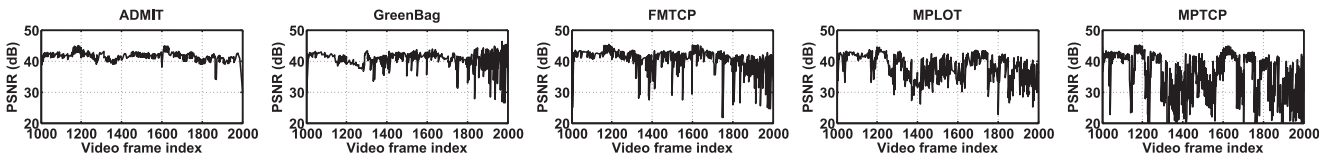

Fig. 8. Comparison of PSNR per video frame measured from the *park joy* sequence.

(a) ADMIT (b) GreenBag (c) FMTCP (d) MPLOT (e) MPTCP

Fig. 9. Comparison of subjective quality measured from *park joy* sequence.

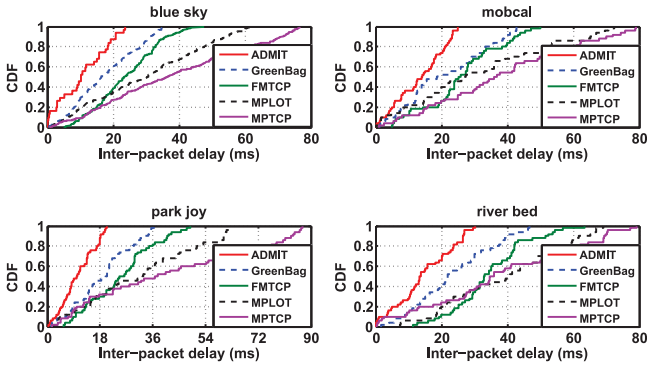

Fig. 11. Cumulative distribution functions (CDF) of inter-packet delay for different sequences.

exhibits superiority in mitigating the transmission losses with the rateless fountain code.

To illustrate the microscopic results of the delay performance, the cumulative distribution functions (CDF) of inter-packet delay (measured at the receiver based on the timestamps of arrival packets) for different video test sequences are shown in Fig. 11. The results indicate ADMIT outperforms the reference schemes in reducing the delay jitters, which may induce frequent playback disruptions. During the video transmission and display process, the receiver side is frequently annoyed with video stalls or glitches while using the reference transport protocols. Much smoother video streaming can be obtained with the proposed ADMIT.

5.2.3 Goodput

Fig. 12a compares the average goodput for the evaluated schemes in the emulations along different mobile trajectories. The performance gaps between ADMIT and the reference schemes become larger in Trajectory III and the results' trend is similar to that shown in Fig. 7a. Another critical problem that degrades the goodput performance is the out-of-order packets, which is mainly caused by the path diversity in heterogeneous networks. The early-arrival packets will be temporarily stored in the receive buffer to wait for the late packets, and this will induce larger end-to-end delay and degrade the channel utilization level. Fig. 7b shows the average percentage of out-of-order packets while the mobile terminal is moving along different trajectories. The risk of packet reordering is obviously higher while the mobile terminal is associated with three access networks in trajectories IV and V. ADMIT succeeds in mitigating the packet reordering problem due to the effectiveness in the rate allocation and delay estimation.

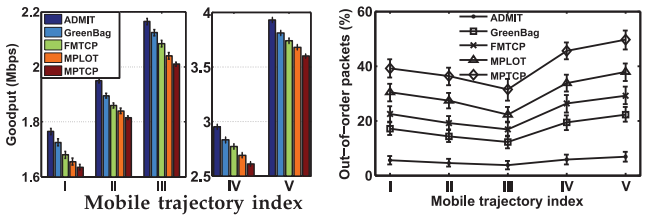

(a) average goodput (b) out-of-order packets

Fig. 12. Comparison of average goodput and out-of-order arrival packets.

Fig. 13a sketches the evolutions of the instantaneous goodput values and it can be observed ADMIT delivers smoother video streaming than the reference transport protocols. This is because the congestion control in MPTCP is a packet-based adaption mechanism and we adjust the FEC packet size to mitigate the throughput fluctuations. In Fig. 13b, we profile the out-of-order arrival packets during the interval of $[0, 400]$ seconds. ADMIT alleviates the packet reordering problem by appropriately selecting the access networks and assigning the transmission rates.

5.3 Componentwise Validation

First, we reveal the effectiveness of the proposed reliability-aware rate allocation algorithm by disabling the FEC adaption component. Fig. 14 compares the PSNR values of the proposed allocation algorithm with those of the packet loss rate based scheme specified in [24]. The results in Fig. 14 verify that the reliability model developed in this work is a better metric than the packet loss rate to indicate the path status for improving overall video streaming quality.

In this emulation scenario, we set the video data to be concurrently transmitted through both cellular and Wi-Fi networks. The evolutions of the total transmission rate and available bandwidth are shown in Fig. 15a. It can be observed the total transmission rate tracks closely to the available bandwidth during the emulations. Such results indicate the FEC coding scheme in ADMIT is able to saturate the communication path to maximize the video quality. In Fig. 15b, we plot the FEC redundancy in comparison to the packet loss rates of Wi-Fi and cellular networks. ADMIT is able to dynamically adjust the redundancy level according to the time-varying packet loss rates to effectively integrate both access networks.

We have also evaluated the impact of congestion losses on the Wi-Fi path. The fairness of ADMIT in this environment is presented in terms of congestion window size (in units of KBytes). We compare the performance of ADMIT with TCP and MPTCP (LIA). There are two video streams

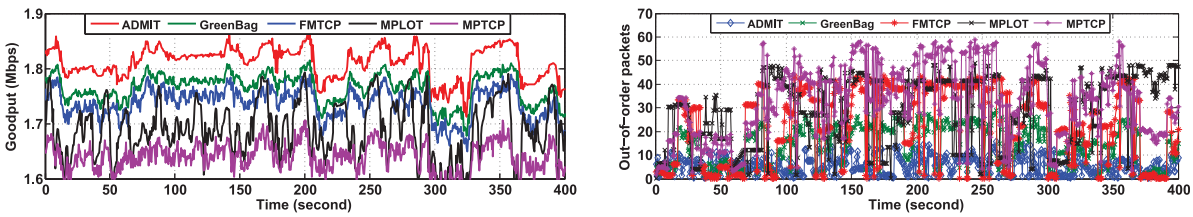

(a) instantaneous goodput values (b) out-of-order arrival packets

Fig. 13. Instantaneous values of goodput and out-of-order arrival packets during the interval of $[0, 400]$ seconds.

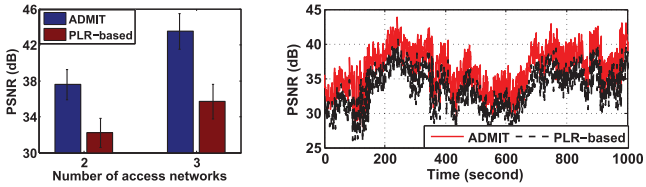

(a) average values (b) instantaneous values

Fig. 14. Effectiveness of the proposed rate allocation algorithm.

in parallel over the Wi-Fi path with one using standard TCP and the other one using ADMIT/MPTCP. The results in Fig. 16 indicate ADMIT flow consumes approximately the same bandwidth that used by the TCP flow. The congestion window size of MPTCP is obviously higher and this is because the Linked Increase Algorithm (LIA) is aggressive toward TCP users [19].

6 Conclusion and Discussion

The exponential growth of mobile video streaming over the Internet has become a major driving force for multihomed communication over heterogeneous wireless networks. Multipath TCP (MPTCP) is an important transport-layer protocol to enable parallel data transmissions over multiple communication paths. This paper proposes ADMIT, a quality-driven MPTCP scheme for multihomed video transmission over multiple wireless access networks. To achieve the optimal quality of real-time video streaming, we first propose a rate allocation algorithm to select the appropriate access networks. Then, we present a FEC coding adaption scheme to strike the balance between end-to-end delay and loss performance to minimize the effective packet loss rate. Emulation results show that ADMIT outperforms the reference transport protocols in improving video quality in terms of PSNR. Furthermore, the superiority of ADMIT over the competing protocols becomes more obvious as the number of access networks increases.

As future work, we will consider the following possible directions.

1) Minimizing the energy consumption of multihomed mobile devices while achieving the target quality to provide user-satisfied video streaming services.
2) Introducing the Quality-of-Experience (QoE) metrics into ADMIT to optimize the video viewing experience.
3) Combining the FEC and retransmission mechanisms in ADMIT (e.g., sending ACK if data is recovered in FEC coding) to reduce unnecessary retransmissions and conserve bandwidth.

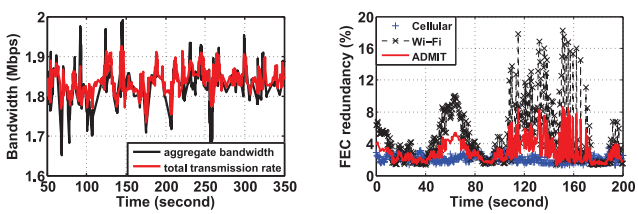

(a) available bandwidth (b) FEC redundancy

Fig. 15. Performance of the FEC coding adaption component.

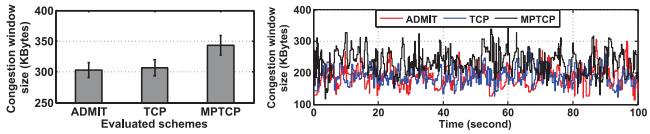

Fig. 16. Fairness results of congestion window size: (a) average value; (b) instantaneous values.

Acknowledgments

This research is partly supported by National Natural Science Foundation of China under Grant No. 61132001; National High-tech R&D Program of China (863 Program) under Grant No. 2013AA102301; Program for New Century Excellent Talents in University (Grant No. NCET-11-0592); and Project of New Generation Broadband Wireless Network under Grant No. 2014ZX03006003; the Multi-plAtform Game Innovation Centre (MAGIC), funded by the Singapore National Research Foundation under its IDM Futures Funding Initiative and administered by the Interactive & Digital Media Programme Office, Media Development Authority. The authors thank the anonymous reviewers and associate editor for their constructive comments to improve the paper quality.

References

[1] J. Lee and S. Bahk, "On the MDP-Based cost minimization for video-on-demand services in a heterogeneous wireless network with multihomed terminals," *IEEE Trans. Mobile Comput.*, vol. 12, no. 9, pp. 1737–1749, Sep. 2013.
[2] J. Wu, B. Cheng, C. Yuen, Y. Shang, and J. Chen, "Distortion-Aware concurrent multipath transfer for mobile video streaming in heterogeneous wireless networks," *IEEE Trans. Mobile Comput.*, vol. 14, no. 4, pp. 689–704, Apr. 2015.
[3] C. Xu, T. Liu, J. Guan, H. Zhang, and G. M. Muntean, "CMT-QA: Quality-Aware adaptive concurrent multipath data transfer in heterogeneous wireless networks," *IEEE Trans. Mobile Comput.*, vol. 12, no. 11, pp. 2193–2205, Nov. 2013.
[4] N. M. Do, C. H. Hsu, and N. Venkatasubramanian, "Video dissemination over hybrid cellular and Ad hoc networks," *IEEE Trans. Mobile Comput.*, vol. 13, no. 2, pp. 274–286, Feb. 2014.
[5] J. Wu, C. Yuen, B. Cheng, Y. Shang, and J. Chen, "Goodput-Aware load distribution for real-time traffic over multipath networks," *IEEE Trans. Parallel Distrib. Syst.*, vol. 26, no. 8, pp. 2286–2299, Aug. 2015.
[6] S. Han, H. Joo, D. Lee, and H. Song, "An end-to-end virtual path construction system for stable live video streaming over heterogeneous wireless networks," *IEEE J. Sel. Areas Commun.*, vol. 29, no. 5, pp. 1032–1041, May 2011.
[7] (2015). [Online]. Available: http://galaxys5guide.com/samsung-galaxy-s5-features-explained/galaxy-s5-download-booster/
[8] (2015). Mushroom networks Inc [Online]. Available: http://www.mushroomnetworks.com/
[9] Y. C. Chen, Y. Lim, R. J. Gibbens, E. M. Nahum, R. Khalili, and D. Towsley, "A Measurement-based study of multipath TCP performance over wireless networks," in *Proc. ACM Conf. Internet Meas. Conf.*, 2013, pp. 455–468.
[10] Y. Lim, Y. C. Chen, E. M. Nahum et al., "Cross-layer path management in multi-path transport protocol for mobile devices," in *Proc. IEEE INFOCOM*, 2014, pp. 1815–1823.
[11] Y. S. Lim, Y. C. Chen, E. M. Nahum, D. Towsley, and K. W. Lee, "Energy-Efficient multipath TCP for mobile devices," in *Proc. 15th ACM Int. Symp. Mobile Ad Hoc Netw. Comput.*, 2014, pp. 257–266.
[12] A. Ford, C. Raiciu, M. Handley, S. Barre, and J. Iyengar, "Architectural guidelines for multipath TCP development," IETF RFC 6182, 2011.
[13] Cisco company, "Cisco visual networking index: Global mobile data traffic forecast update, 2014-2019," Feb. 2015.
[14] (2015). Web Real-Time Communication [Online]. Available: http://www.webrtc.com/

[15] (2015). HTTP live streaming [Online]. Available: https://developer.apple.com/streaming/
[16] J. Wu, C. Yuen, N.-M. Cheung, J. Chen, and C. W. Chen, "Enabling adaptive high-frame-rate video streaming in mobile cloud gaming applications," *IEEE Trans. Circuits Syst. Video Technol.*, to be published, Doi: 10.1109/TCSVT.2015.2441412.
[17] H. Schulzrinne, S. Casner, R. Frederick, and V. Jacobson, "RTP: A transport protocol for real-time applications," IETF RFC 3550, 2003.
[18] H. Schulzrinne, A. Rao, and R. Lanphier, "Real time streaming protocol (RTSP)," IETF RFC 2326, 1998.
[19] R. Khalili, N. Gast, M. Popovic, U. Upadhyay, and J. Boudec, "MPTCP is not pareto-optimal: Performance issues and a possible solution," *IEEE/ACM Trans. Netw.*, vol. 21, no. 5, pp. 1651–1665, Oct. 2013.
[20] E. Brosh, S. A. Baset, V. Misra, D. Rubenstein, and H. Schulzrinne, "The delay-friendliness of TCP for real-time traffic," *IEEE/ACM Trans. Netw.*, vol. 18, no. 5, pp. 1478–1491, Oct. 2010.
[21] Y. Cui, L. Wang, X. Wang, H. Wang, and Y. Wang, "FMTCP: A fountain code-based multipath transmission control protocol," *IEEE/ACM Trans. Netw.*, vol. 23, no. 2, pp. 465–478, Apr. 2015.
[22] D. Wischik, C. Raiciu, A. Greenhalgh, and M. Handley, "Design, implementation and evaluation of congestion control for multipath TCP," in *Proc. 8th USENIX Conf. Netw. Syst. Des. Implementation*, 2011, pp. 99–112.
[23] J. Wu, C. Yuen, and J. Chen, "Leveraging the delay-friendliness of TCP with FEC coding in real-time video communication," *IEEE Trans. Commun.*, vol. 63, no. 10, pp. 3584-3599, Oct. 2015.
[24] C. Raiciu, M. Handley, and D. Wischik, "Coupled congestion control for multipath transport protocols," IETF RFC 6356, 2011.
[25] D. H. Bui, K. Lee, S. Oh, I. Shin, H. Shin, H. Woo, and D. Ban, "Greenbag: Energy-efficient bandwidth aggregation for real-time streaming in heterogeneous mobile wireless networks," in *Proc. IEEE 34th Real-Time Syst. Symp.*, 2013, pp. 57–67.
[26] V. Sharma, K. Kar, K. K. Ramakrishnan, and S. Kalyanaraman, "A transport protocol to exploit multipath diversity in wireless networks," *IEEE/ACM Trans. Netw.*, vol. 20, no. 4, pp. 1024–1039, Aug. 2012.
[27] J. Wu, J. Yang, X. Wu, and J. Chen, "A low latency scheduling approach for high definition video streaming over heterogeneous wireless networks," in *Proc. IEEE GLOBECOM*, 2013, pp. 1723–1729.
[28] W. Song and W. Zhuang, "Performance analysis of probabilistic multipath transmission of video streaming traffic over multi-radio wireless devices," *IEEE Trans. Wireless Commun.*, vol. 11, no. 4, pp. 1554–1564, Apr. 2012.
[29] J. Wu, Y. Shang, J. Huang, X. Zhang, B. Cheng, and J. Chen, "Joint source-channel coding and optimization for mobile video streaming in heterogeneous wireless networks," *EURASIP J. Wireless Commun. Netw.*, vol. 2013, pp. 1–16, 2013.
[30] J. Wu, Y. Shang, B. Cheng, B. Wu, and J. Chen, "Loss tolerant bandwidth aggregation for multihomed video streaming over heterogeneous wireless networks," *Wireless Personal Commun.*, vol. 75, no. 2, pp. 1265–1282, 2014.
[31] O. Bonaventure. (2015). Multipath TCP: An annotated bibliography [Online]. Available: http://blog.multipath-tcp.org/blog/html/2015/04/09/bibliography.html
[32] A. Ford, C. Raiciu, M. Handley, and O. Bonaventure, "TCP extensions for multipath operation with multiple addresses," IETF RFC 6824, 2013.
[33] M. Li, A. Lukyanenko, S. Tarkoma, Y. Cui, and A. Yla-Jaaski, "Tolerating path heterogeneity in multipath TCP with bounded receive buffers," *Comput. Netw.*, vol. 64, pp. 1–14, 2013.
[34] J. Wu, C. Yuen, M. Wang, and J. Chen, "Content-Aware concurrent multipath transfer for high-definition video streaming over heterogeneous wireless networks," *IEEE Trans. Parallel Distrib. Syst.*, to be published, Doi: 10.1109/TPDS.2015.2416736.
[35] S. Deng, R. Netravali, A. Sivaraman, and H. Balakrishnan, "Wi-Fi, LTE, or Both?: Measuring multi-homed wireless internet performance," in *Proc. ACM Conf. Internet Meas. Conf.*, 2014, pp. 181–194.
[36] K. Stuhlmüller, N. Färber, M. Link, and B. Girod, "Analysis of video transmission over lossy channels," *IEEE J. Sel. Areas Commun.*, vol. 18, no. 6, pp. 1012–1032, Jun. 2000.
[37] P. Frossard, "FEC performances in multimedia streaming," *IEEE Commun. Lett.*, vol. 5, no. 3, pp. 122–124, Mar. 2001.
[38] M. Jain and C. Dovrolis, "End-to-end available bandwidth: Measurement methodology, dynamics, and relation with TCP throughput," *IEEE/ACM Trans. Netw.*, vol. 11, no. 4, pp. 537–549, Aug. 2003.
[39] E. Gilbert, "Capacity of a burst-noise channel," *Bell Syst. Tech. J.*, vol. 39, no. 9, pp. 1253–1265, 1960.
[40] G. Hasslinger, A. Schwahn, and F. Hartleb, "2-State (semi-) Markov processes beyond Gilbert-Elliott: Traffic and channel models based on 2nd order statistics," in *Proc. IEEE INFOCOM*, 2013, pp. 1438–1446.
[41] Y. Xu, C. Yu, J. Li, and Y. Liu, "Video telephony for end-consumers: Measurement study of Google+, iChat, and Skype," *IEEE/ACM Trans. Netw.*, vol. 22, no. 3, pp. 826–839, Jun. 2014.
[42] X. Zhang, Y. Xu, H. Hu, Y. Liu, Z. Guo, and Y. Wang, "Profiling skype video calls: Rate control and video quality," in *Proc. IEEE INFOCOM*, 2012, pp. 621–629.
[43] C. P. Fu and S. C. Liew, "TCP Veno: TCP enhancement for transmission over wireless access networks," *IEEE J. Sel. Areas Commun.*, vol. 21, no. 2, pp. 216–228, Feb. 2003.
[44] S. Cen, P. C. Cosman, and G. M. Voelker, "End-to-end differentiation of congestion and wireless losses," *IEEE/ACM Trans. Netw.*, vol. 11, no. 5, pp. 703–717, Oct. 2003.
[45] X. Zhu, P. Agrawal, J. P. Singh, T. Alpcan, and B. Girod, "Distributed rate allocation policies for multihomed video streaming over heterogeneous access networks," *IEEE Trans. Multimedia*, vol. 11, no. 4, pp. 752–764, Jun. 2009.
[46] J. Nagle, "Congestion control in IP/TCP Internetworks," IETF RFC 896, 1984.
[47] L. Zhou, H. Wang, S. Lian, Y. Zhang, A. Vasilakos, and W. Jing, "Availability-aware multimedia scheduling in heterogeneous wireless networks," *IEEE Trans. Veh. Technol.*, vol. 60, no. 3, pp. 1161–1170, Mar. 2011.
[48] J. Wu, Y. Shang, X. Qiao, B. Cheng, and J. Chen, "Robust bandwidth aggregation for real-time video delivery in integrated heterogeneous wireless networks," *Multimedia Tools Appl.*, vol. 74, no. 11, pp. 4117–4138, 2015.
[49] G. Auwera and M. Reisslein, "Implications of smoothing on statistical multiplexing of H. 264/AVC and SVC video streams," *IEEE Trans. Broadcast.*, vol. 55, no. 3, pp. 541–558, Sep. 2009.
[50] T. Hartman, A. Hassidim, H. Kaplan, D. Raz, and M. Segalov, "How to split a flow?" in *Proc. of IEEE INFOCOM*, 2012, pp. 828–836.
[51] T. Oliveira, S. Mahadevan, and D. P. Agrawal, "Handling network uncertainty in heterogeneous wireless networks," in *Proc. IEEE INFOCOM*, 2011, pp. 2390–2398.
[52] J. Wu, C. Yuen, N.-M. Cheung, and J. Chen, "Delay-Constrained high definition video transmission in heterogeneous wireless networks with multi-homed terminals," *IEEE Trans. Mobile Comput.*, to be published, Doi: 10.1109/TMC.2015.2426710.
[53] X. Qin and T. Xie, "An availability-aware task scheduling strategy for heterogeneous systems," *IEEE Trans. Comput.*, vol. 57, no. 2, pp. 188–199, Feb. 2008.
[54] V. Singh, S. Ahsan, and J. Ott, "MPRTP: Multipath considerations for real-time media," in *Proc. 4th ACM Multimedia Syst. Conf.*, 2013, pp. 190–201.
[55] F. Kelly and T. Voice, "Stability of end-to-end algorithm for joint routing and rate control," *ACM SIGCOMM Comput. Commun. Rev.*, vol. 32, no. 2, pp. 5-12, 2005.
[56] (2014). [Online]. Available: http://www.scalable-networks.com/exata
[57] (2014). [Online]. Available: http://www.scalable-networks.com/qualnet
[58] J. Huang, F. Qian, A. Gerber, Z. M. Mao, S. Sen, and O. Spatscheck, "A close examination of performance and power characteristics of 4G LTE networks," in *Proc. ACM 10th Int. Conf. Mobile Syst., Appl. Serv.*, 2012, pp. 225–238.
[59] (2015). [Online]. Available: https://github.com/multipath-tcp/mptcp/
[60] J. Wu, J. Yang, Y. Shang, B. Cheng, and J. Chen, "SPMLD: Subpacket based multipath load distribution for real-time multimedia traffic," *J. Commun. Netw.*, vol. 16, no. 5, pp. 548-558, 2014.
[61] (2014). [Online]. Available: http://iphome.hhi.de/suehring/tml/
[62] ANSI (American National Standards Institute) T1.TR.74-2001, "Objective video quality measurement using a peak-signal-to-noise-ratio (PSNR) full reference technique," 2001.
[63] J. Wu, B. Cheng, C. Yuen, N.-M. Cheung, and J. Chen, "Trading delay for distortion in one-way video communication over the internet," *IEEE Trans. Circuits Syst. Video Technol.*, to be published, Doi: 10.1109/TCSVT.2015.2412774.

Jiyan Wu received the bachelor's degree from the North China Institute of Science and Technology in June 2008, the master's degree from the China University of Mining and Technology, Beijing, China, in June 2011, and the PhD degree in computer science and technology from the Beijing University of Posts and Telecommunications (supervisor: Prof. Junliang Chen) in June 2014. He is currently working as a senior software engineer with the Department of Research and Development, OmniVision Technologies Singapore Pte. Ltd., and also as an adjunct researcher with the Research Institute of Networking Technology, Beijing University of Posts and Telecommunications. He was a postdoctoral research fellow from March 2014 to January 2016 with Singapore University of Technology and Design, Singapore, and a software developer (C++) from October 2010 to February 2014 with Sinosoft Technologies Co. Ltd., Beijing, China. His research interests include video communication, video coding, forward error correction, heterogeneous wireless networks, and concurrent multipath transfer. His programming experiences/interests include client-server video communication, peer-to-peer mobile data transfer, real-time data system, and back-end server programs. He is a member of the IEEE.

Chau Yuen received the BEng and PhD degrees from Nanyang Technological University, Singapore, in 2000 and 2004, respectively. He was a postdoc fellow at Lucent Technologies Bell Labs, Murray Hill in 2005. He was also a visiting assistant professor at Hong Kong Polytechnic University in 2008. During the period of 2006 to 2010, he was at the Institute for Infocomm Research, Singapore, as a senior research engineer. He joined the Singapore University of Technology and Design as an assistant professor in June 2010. He also serves as an associate editor for *IEEE Transactions on Vehicular Technology*. In 2012, he received the IEEE Asia-Pacific Outstanding Young Researcher Award. He is a senior member of the IEEE.

Bo Cheng received the PhD degree in computer science and engineering in July 2006, from the University of Electronic Science and Technology of China. He has been working in the Beijing University of Posts and Telecommunications (BUPT) since 2008. He is now a professor of the Research Institute of Networking Technology of BUPT. His current research interests include network services and intelligence, Internet of Things technology, communication software and distribute computing, etc. He is a member of the IEEE.

Ming Wang received the master's degree from the University of Science and Technology Beijing (USTB) in January 2011. He is currently working toward the PhD degree in computer science and technology in the State Key Laboratory of Networking and Switching Technology, Beijing University of Posts and Telecommunications (BUPT). His research interests include multimedia networking and media processing.

Junliang Chen received the BS degree in electrical engineering from Shanghai Jiaotong University, China, in 1955 and the PhD degree in electrical engineering in May, 1961, from the Moscow Institute of Radio Engineering, formerly Soviet Russia. He is the chairman and a professor of the Research Institute of Networking and Switching Technology at the Beijing University of Posts and Telecommunications (BUPT). He has been working at BUPT since 1955. His research interests are in the area of communication networks and next generation service creation technology. He was elected as a member of the Chinese Academy of Science in 1991, and a member of the Chinese Academy of Engineering in 1994, for his contributions to fault diagnosis in stored program control exchange. He received the first, second, and third prizes of National Scientific and Technological Progress Award in 1988, 2004, and 1999, respectively.